

# Efficient Techniques for Shape Optimization with Variational Inequalities using Adjoints

Daniel Luft\*    Volker Schulz†    Kathrin Welker‡

December 20, 2024

## Abstract

In general, standard necessary optimality conditions cannot be formulated in a straightforward manner for semi-smooth shape optimization problems. In this paper, we consider shape optimization problems constrained by variational inequalities of the first kind, so-called obstacle-type problems. Under appropriate assumptions, we prove existence of adjoints for regularized problems and convergence to adjoints of the unregularized problem. Moreover, we derive shape derivatives for the regularized problem and prove convergence to a limit object. Based on this analysis, an efficient optimization algorithm is devised and tested numerically.

**Key words:** Semi-smooth optimization, variational inequality, obstacle problem, shape optimization, numerical methods, adjoint methods.

**AMS subject classifications:** 65K15, 49Q10, 49M29, 35Q93, 35J86, 49J40.

## 1 Introduction

We consider shape optimization problems constrained by variational inequalities (VI) of the first kind, so-called obstacle-type problems. Applications arise, whenever a shape is to be constructed in a way not to violate constraints for the state solutions of partial differential equation depending on a geometry to be optimized. Just think of a heat equation depending on a shape, where the temperature is not allowed to surpass a certain threshold. This example is basically the model problem that we are formulating in section 2.

Shape optimization problem constraints in the form of VIs are challenging, since classical constraint qualifications for deriving Lagrange multipliers generically fail. Therefore, not only the development of stable numerical solution schemes but also the development of suitable first order optimality conditions is an issue.

By usage of tools of modern analysis, such as monotone operators in Banach spaces, significant results on properties of solution operators of variational inequalities have been achieved since the 1960s (cf. [5, 6, 26]). However, there are only very few approaches in literature to the problem class of VI constrained shape optimization problems so far. In [25], shape optimization of 2D elasto-plastic bodies is studied, where the shape is simplified to a graph such that one dimension can be

\*Trier University, Department of Mathematics, 54286 Trier, Germany ([luft@uni-trier.de](mailto:luft@uni-trier.de))

†Trier University, Department of Mathematics, 54286 Trier, Germany ([volker.schulz@uni-trier.de](mailto:volker.schulz@uni-trier.de))

‡Helmut Schmidt University / University of the Federal Armed Forces, Faculty of Mechanical Engineering, 22043 Hamburg, Germany ([welker@hsu-hh.de](mailto:welker@hsu-hh.de))

written as a function of the other. The non-trivial existence of solutions of VI constrained shape optimization problems is discussed in [10, 38]. E.g., in [38, Chap. 4], shape derivatives of elliptic variational inequality problems are presented in the form of solutions to again variational inequalities. In [31], shape optimization for 2D graph-like domains are investigated. Also [27, 28] present existence results for shape optimization problems which can be reformulated as optimal control problems, whereas [12, 15] show existence of solutions in a more general set-up. In [32, 33], level-set methods are proposed and applied to graph-like two-dimensional problems. Moreover, [19] presents a regularization approach to the computation of shape and topological derivatives in the context of elliptic variational inequalities and, thus, circumventing the numerical problems in [38, Chap. 4]. Recently, in [16], a sensitivity analysis is performed for a class of semi-linear variational inequalities and a strong convergence property is shown for the material derivative. Furthermore, state-shape derivatives are established under regularity assumptions.

In this paper, we aim at optimality conditions for VI constrained shape optimization in the flavor of optimality conditions for VI constrained optimal control problems as in [17, 18, 20]. In general, standard necessary optimality conditions cannot be formulated in a straightforward manner for semi-smooth shape optimization problems. Under appropriate assumptions, we prove existence of adjoints and convergence of adjoints resulting from regularized variational inequalities. These analytical results are also verified numerically. Moreover, convergence of shape derivatives related to the smoothed problem is shown and the limit object is identified. Furthermore, we build on the resulting optimality conditions and devise an optimization algorithm giving specific numerical results. This algorithm does no longer depend on smoothing strategies as in [14]. In [14], a shape optimization method based on a regularized variant of the variational inequality has been devised and observed that the performance of this algorithm strongly depends on the tightness of the obstacle. This problem does no longer arise with the strategy developed in the present paper. On the contrary, the algorithms gets even faster, the more degrees of freedom are constrained by the obstacle.

This paper is structured as follows. In section 2, we formulate the VI constrained shape optimization model with general elliptic coefficients on which we focus in this paper. The necessary optimality conditions, including the existence of adjoint variables under certain regularity assumptions to the model problem are formulated in section 3. In section 4, we formulate an algorithm to solve the model problem based on these analytical results and compare numerically this approach with several regularized strategies.

## 2 Problem class

Let  $\Omega \subset \mathbb{R}^2$  be a bounded domain equipped with a sufficiently smooth boundary  $\partial\Omega$ . This domain is assumed to be partitioned in a subdomain  $\Omega_{\text{out}} \subset \Omega$  and an interior domain  $\Omega_{\text{int}} \subset \Omega$  with boundary  $\Gamma_{\text{int}} := \partial\Omega_{\text{int}}$  such that  $\Omega_{\text{out}} \sqcup \Omega_{\text{int}} \sqcup \Gamma_{\text{int}} = \Omega$ , where  $\sqcup$  denotes the disjoint union. The closure of  $\Omega$  is denoted by  $\bar{\Omega}$ . We consider  $\Omega$  depending on  $\Gamma_{\text{int}}$ , i.e.,  $\Omega = \Omega(\Gamma_{\text{int}})$ . Figure 1 illustrates this situation. In the following, the boundary  $\Gamma_{\text{int}}$  of the interior domain is called the *interface* and an element of an appropriate shape space  $\mathcal{X}$  (cf. remark 1). In contrast to the outer boundary  $\partial\Omega$ , which is assumed to be fixed, the inner boundary  $\Gamma_{\text{int}}$  is variable. If  $\Gamma_{\text{int}}$  changes, then the subdomains  $\Omega_{\text{int}}, \Omega_{\text{out}} \subset \Omega$  change in a natural manner.

Let  $\nu > 0$  be an arbitrary constant. For the objective function

$$J(y, \Omega) := \mathcal{J}(y, \Omega) + \mathcal{J}_{\text{reg}}(\Omega) := \frac{1}{2} \int_{\Omega} |y - \bar{y}|^2 dx + \nu \int_{\Gamma_{\text{int}}} 1 ds \quad (1)$$

we consider the following shape optimization problem:

$$\min_{\Gamma_{int} \in \mathcal{X}} J(y, \Omega) \quad (2)$$

constrained by the following obstacle type variational inequality:

$$a(y, v - y) \geq \langle f, v - y \rangle \quad \forall v \in K := \{\theta \in H_0^1(\Omega) : \theta(x) \leq \varphi(x) \text{ in } \Omega\}, \quad (3)$$

where  $y \in K$  is the solution of the VI,  $f \in L^2(\Omega)$  is explicitly dependent on the shape,  $\langle \cdot, \cdot \rangle$  denotes the duality pairing and  $a(\cdot, \cdot)$  is a general elliptic bilinear form

$$\begin{aligned} a: H_0^1(\Omega) \times H_0^1(\Omega) &\rightarrow \mathbb{R} \\ (y, v) &\mapsto \sum_{i,j} a_{i,j} \partial_i y \partial_j v + \sum_i d_i (\partial_i y v + y \partial_i v) + b y v \end{aligned} \quad (4)$$

defined by coefficient functions  $a_{i,j}, d_j, b \in L^\infty(\Omega)$ .

With the tracking-type objective  $\mathcal{J}$  the model is fitted to data measurements  $\bar{y} \in L^2(\Omega)$ . The second term  $\mathcal{J}_{reg}$  in the objective function  $J$  is a perimeter regularization. A perimeter regularization is frequently used to overcome ill-posedness of shape optimization problems, e.g., [2] investigates the regularization and numerical solution of geometric inverse problems related to linear elasticity. In eq. (3),  $\varphi$  denotes an obstacle which needs to be an element of  $L_{loc}^1(\Omega)$  such that the set of admissible functions  $K$  is non-empty (cf. [38]). If additionally  $\partial\Omega$  is  $C^{1,1}$  or a polyhedron and  $\varphi \in H^2(\Omega)$ , then the solution to eq. (3) satisfies  $y \in H_0^1(\Omega)$ , given that the assumptions from above hold, see, e.g., [22] Remark 2.3. (cf. [21, 9, 41]). Further, eq. (3) can be equivalently expressed as

$$a(y, v) + (\lambda, v)_{L^2(\Omega)} = (f, v)_{L^2(\Omega)} \quad \forall v \in H_0^1(\Omega) \quad (5)$$

$$\begin{aligned} \lambda &\geq 0 \quad \text{in } \Omega \\ y &\leq \varphi \quad \text{in } \Omega \\ \lambda(y - \varphi) &= 0 \quad \text{in } \Omega \end{aligned} \quad (6)$$

with  $(\cdot, \cdot)_{L^2(\Omega)}$  denoting the  $L^2$ -scalar product and  $\lambda \in L^2(\Omega)$ .

It is well-known, e.g., from [9], that under these assumptions there exists a unique solution  $y$  to the obstacle type variational inequality (3) and an associated Lagrange multiplier  $\lambda$ . The existence of solutions of any shape optimization problem is a non-trivial question. Shape optimization problems constrained by VIs are especially challenging because, in general, it is not guaranteed that an adjoint state can be introduced (cf. [38, Example in Chap. 1, Chap. 4]). An essential theoretical tool for the study of the existence of solutions is the derivation of optimality conditions, i.e., in particular, the formulation of an adjoint equation. Therefore, section 3 investigates the model problem analytically, also in view of formulating a numerically applicable algorithm in section 4.

**Remark 1.** *The interface  $\Gamma_{int}$  is an element of an appropriate shape space. Please note that there exists no common shape space suitable for all applications. The modeling of a shape space is a challenging task and different approaches lead to diverse models. There is a multitude of shape spaces in the literature like landmark vectors, plane curves, surfaces, multiphase objects, characteristic functions of measurable sets, morphologies of images, etc. From a computational point of view one has to deal with polygonal shape representations arising in the setting of constrained shape optimization. This is owed to the fact that finite element methods usually discretize*

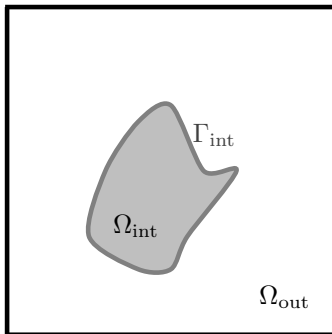


Figure 1: Example of a domain  $\Omega = \Omega_{\text{out}} \sqcup \Gamma_{\text{int}} \sqcup \Omega_{\text{int}}$ .

the models. In this paper, we use these methods and, thus, the space of  $H^{1/2}$ -shapes investigated in [43] together with the Steklov-Poincaré metric defined in [36] as a possible choice for a shape space. In [37], it is outlined that this is an essential step towards applying efficient FE solvers. Of course, it is possible to choose other shape space models but this is beyond the scope of this paper.

### 3 Convergence results for adjoints and shape derivatives

The direct handling of obstacle-type variational inequalities formulated as in (5)-(6) poses several problems. One problem is that in general the multiplier  $\lambda$  is only element of  $H^{-1}(\Omega)$ , leading to severe numerical challenges. Under the assumptions mentioned in section 2, which are also found in [22], we have  $\lambda \in L^2(\Omega)$ , meaning that we have a representation of the distribution as a  $L^2$ -function. It can be easily verified that this in turn gives the possibility to summarize the conditions (6) equivalently into a single condition of the form

$$\lambda = \max(0, \lambda + c(y - \varphi)) \quad \text{for any } c > 0. \quad (7)$$

This formulation still leaves us with the difficulty of finding such a multiplier. For this reason, a regularization is often employed by substitution of  $\lambda \in L^2(\Omega)$  by an independent  $\bar{\lambda} \in L^2(\Omega)$ . This results in the equation

$$a(y_c, v) + (\max(0, \bar{\lambda} + c(y_c - \varphi)), v)_{L^2(\Omega)} = (f, v)_{L^2(\Omega)} \quad \forall v \in H_0^1(\Omega), \quad (8)$$

which in the following is called *regularized state equation* or *regularized obstacle problem*. Explicit dependence on  $\lambda$  is avoided, making the resulting semi-linear elliptic equation tractable, for example by semi-smooth Newton methods, see, e.g., [22]. Moreover, the authors of [22] prove  $L^2$ -convergence of the regularized multiplier  $\max(0, \bar{\lambda} + c \cdot (y_c - \varphi))$  to the original  $\lambda$  for their method.

With problem (8) we are still left to solve a nonlinear, semi-smooth problem, giving rise to problems concerning existence of adjoints. Hence, standard smoothing strategies can be applied to render this problem smooth enough to show existence of adjoints and to apply techniques such as Newton iterations.

In light of [35] and [7], we pose the following assumptions on the smoothed max-function, which from now on is called  $\max_\gamma: \mathbb{R} \rightarrow [0, \infty)$ , with  $\gamma > 0$  being the smoothing parameter:

**Assumption 1** (on smoothed max-function).

(i)  $\max_\gamma \in C^1(\Omega)$  for all  $\gamma > 0$ ;

(ii) there exists a function  $g: (0, \infty) \rightarrow [0, \infty)$  with  $g(\gamma) \rightarrow 0$  as  $\gamma \rightarrow \infty$ , s.t.  $|\max_\gamma(x) - \max(0, x)| \leq g(\gamma)$  for all  $x \in \mathbb{R}$  and for all  $\gamma > 0$ ;

(iii)  $\max'_\gamma(x) \in [0, 1]$  and monotonically nondecreasing for all  $x \in \mathbb{R}$  and all  $\gamma > 0$ ;

(iv)  $\max'_\gamma$  converges uniformly to 0 on  $(-\infty, -\delta)$  and 1 on  $(\delta, \infty)$  for all  $\delta > 0$  for  $\gamma \rightarrow \infty$ .

In the following, let  $\text{sign}_\gamma$  denote the derivative of  $\max_\gamma$ . An example satisfying these assumptions is given in (41). Applying  $\max_\gamma$  instead of  $\max$  in (8) gives the following equation, which we call *fully regularized state equation* in the subsequent chapters:

$$a(y_{\gamma,c}, v) + (\max_\gamma(\bar{\lambda} + c(y_{\gamma,c} - \varphi)), v)_{L^2(\Omega)} = (f, v)_{L^2(\Omega)} \quad \forall v \in H_0^1(\Omega). \quad (9)$$

So linearizing the corresponding Lagrangian with respect to  $y_{\gamma,c}$  results in the typical adjoint equation

$$\begin{aligned} a(p_{\gamma,c}, v) + c \cdot (\text{sign}_\gamma(\bar{\lambda} + c(y_{\gamma,c} - \varphi)) \cdot p_{\gamma,c}, v)_{L^2(\Omega)} \\ = -(y_{\gamma,c} - \bar{y}, v)_{L^2(\Omega)} \quad \forall v \in H_0^1(\Omega) \end{aligned} \quad (10)$$

(see, e.g., [17] or [35] in the context of optimal control).

**Remark 2.** As in [35], smoothness of the state equation (9) in  $y_{\gamma,c}$  guarantees existence of solutions to the linearized equation (10) for a given  $L^2(\Omega)$  right-hand side and, thus, existence of adjoints in the case of the considered tracking-type objective functional (1).

### 3.1 State and adjoint equation

We first show that solutions of eq. (9) converge strongly in  $H^1$  to solutions of (5)-(6) for  $\gamma, c \rightarrow \infty$ . This is proven in [35] for stronger assumptions on the smoothed function  $\max_\gamma$  and under  $\gamma = c$ . Since we rely on the general case  $\gamma \neq c$  for the proofs in ongoing discussions, we state an according result. The first part of the following theorem is in analogy to [7, Lemma 4.2]. However, the difference is that we consider general elliptic bilinear forms and—more importantly—a modified argument in the maximum function resulting in different regularized state equations. These generalizations are necessary for our further analytical investigations leading to an adjoint equation.

**Proposition 1** ( $H^1$ -convergence of the state). *Let  $y_{\gamma,c}$ ,  $y_c$  and  $y$  be solutions to eq. (9), eq. (8) and eq. (5), respectively. Here,  $a(\cdot, \cdot)$  is chosen by an elliptic bilinear form as in (4) on a compact domain  $\Omega$  with polyhedral or  $C^{1,1}$ -boundary,  $f \in L^2(\Omega)$  and  $\gamma, c > 0$ . Moreover, assume  $\varphi \in H^2(\Omega)$ ,  $\bar{\lambda} \in L^2(\Omega)$  and let  $\max_\gamma: \mathbb{R} \rightarrow \mathbb{R}$  satisfy assumption 1. Then*

$$y_{\gamma,c} \rightarrow y_c \text{ in } H^1(\Omega) \quad \text{as } \gamma \rightarrow \infty; \quad (11)$$

$$y_c \rightarrow y \text{ in } H^1(\Omega) \quad \text{as } c \rightarrow \infty. \quad (12)$$

*Proof.* We prove the first statement (11) of the theorem. For a proof of the second statement (12), we refer to [22, Theorem 3.1].

We start by ensuring the existence of solutions to eq. (9) and eq. (8). For this, we show that the Nemetskii-operator defined by

$$\Phi_\gamma: H^1(\Omega) \rightarrow L^2(\Omega), y \mapsto \max_\gamma(\bar{\lambda} + c \cdot (y - \varphi)) \quad (13)$$

is a monotone operator for all  $\gamma, c > 0$ . Due to assumption 1, it is clear that  $\max_\gamma: \mathbb{R} \rightarrow \mathbb{R}$  is a point-wise monotone function, implying that  $\max_\gamma: H^1(\Omega) \rightarrow H^1(\Omega), y \mapsto \max_\gamma(y)$  is a monotone operator. Since

$$\Psi_c: H^1(\Omega) \rightarrow H^1(\Omega), y \mapsto \bar{\lambda} + c \cdot (y - \varphi)$$

is an affine linear operator, and, thus monotone, the composition  $\max_\gamma \circ \Psi_c = \Phi_\gamma$  is also monotone. The same argument holds for the non-smoothed operator

$$\Phi: H^1(\Omega) \rightarrow L^2(\Omega), y \mapsto \max(0, \bar{\lambda} + c \cdot (y - \varphi)).$$

Therefore, applying the Browder-Minty theorem for monotone operators yields the existence of solutions to eq. (9) and eq. (8) in  $H^1(\Omega)$  for all  $f \in L^2(\Omega)$  if  $\Omega$  is bounded and we operate in Hilbert spaces.

Now, we prove the second convergence (11). For fixed  $c > 0$ , let  $y_{\gamma,c}$  and  $y_c$  be solutions to eq. (9) and eq. (8), respectively. Assumption 1 (ii) together with the monotonicity of  $\Phi$ , the coercivity of  $a(\cdot, \cdot)$  with constant  $\kappa > 0$  and  $y_{\gamma,c} - y_c \in H^1(\Omega)$  acting as a test-function yields

$$\begin{aligned} 0 &\leq \kappa \cdot \|y_{\gamma,c} - y_c\|_{H^1(\Omega)}^2 \\ &\leq a(y_{\gamma,c} - y_c, y_{\gamma,c} - y_c) \\ &\leq a(y_{\gamma,c} - y_c, y_{\gamma,c} - y_c) \\ &\quad + \left( \max(0, \bar{\lambda} + c(y_{\gamma,c} - \varphi)) - \max(0, \bar{\lambda} + c(y_c - \varphi)), y_{\gamma,c} - y_c \right)_{L^2(\Omega)} \\ &= \left( \max_\gamma(\bar{\lambda} + c(y_{\gamma,c} - \varphi)) - \max(0, \bar{\lambda} + c(y_{\gamma,c} - \varphi)), y_{\gamma,c} - y_c \right)_{L^2(\Omega)} \\ &\leq \int_\Omega |\max_\gamma(\bar{\lambda} + c(y_{\gamma,c} - \varphi)) - \max(0, \bar{\lambda} + c(y_{\gamma,c} - \varphi))| \cdot |y_{\gamma,c} - y_c| \, dx \\ &\leq g(\gamma) \cdot \text{vol}(\Omega) \cdot \|y_{\gamma,c} - y_c\|_{H^1(\Omega)}, \end{aligned}$$

which gives the desired convergence (11).  $\square$

The following definition is needed to state the first main result of this paper, the convergence of adjoints.

**Definition 1.** Let  $\Omega \subset \mathbb{R}^n$  be a bounded, open domain with Lipschitz boundary. A set  $A \subseteq \Omega$  is called regularly decomposable, if there exists an  $N \in \mathbb{N}$  and disjoint, path-connected and closed  $A_i \subset \Omega$  with Lipschitz boundaries  $\partial A_i$  such that  $A = \bigsqcup_{i=1}^N A_i$ .

With this definition it is possible to formulate the first main theorem concerning the convergence of adjoints corresponding to the fully regularized problems and characterization of the limit object.

**Theorem 1** (Convergence of the adjoints). Let  $\Omega \subset \mathbb{R}^2$  be a bounded, open domain with  $C^2$ -boundary. Moreover, let the following assumptions are satisfied:

- (i)  $\varphi \in H^2(\Omega)$ ,  $f \in L^2(\Omega)$ , and coefficient functions  $a_{i,j}, d_j, b \in L^\infty(\Omega)$  in (5)-(6);
- (ii) the active set  $A = \{x \in \Omega \mid y - \varphi \geq 0\}$  corresponding to (5)-(6) is regularly decomposable;

(iii)  $A_c := \{x \in \Omega \mid \bar{\lambda} + c \cdot (y_c - \varphi) \geq 0\}$  is regularly decomposable and

$$A_c \subseteq A \quad \forall c > 0, \quad (14)$$

where  $y_c$  solves the regularized state equation (8);

(iv) the following convergence holds:

$$\|\text{sign}_\gamma(\bar{\lambda} + c \cdot (y_{\gamma,c} - \varphi)) - \text{sign}(\bar{\lambda} + c \cdot (y_c - \varphi))\|_{L^1(\Omega)} \rightarrow 0 \quad \text{for } \gamma \rightarrow \infty. \quad (15)$$

Then the adjoints  $p_{\gamma,c} \rightarrow p_c$  in  $H_0^1(\Omega)$  for  $\gamma \rightarrow \infty$  for all  $c > 0$ , where  $p_c$  is the solution to

$$a(p_c, v) + c \cdot \int_{\Omega} \mathbb{1}_{A_c} \cdot p_c \cdot v \, dx = - \int_{\Omega} (y_c - \bar{y}) \cdot v \, dx \quad \forall v \in H_0^1(\Omega). \quad (16)$$

Moreover, there exists  $p \in H^{-1}(\Omega)$  to (5)-(6) and  $p$  is representable as an  $H_0^1$ -function given by the extension of  $\tilde{p} \in H_0^1(\Omega \setminus A)$  to  $\Omega$ , i.e.,

$$p = \begin{cases} \tilde{p} & \text{in } \Omega \setminus A \\ 0 & \text{in } A \end{cases}, \quad (17)$$

where  $\tilde{p} \in H_0^1(\Omega \setminus A)$  is the solution of the elliptic problem

$$a_{\Omega \setminus A}(\tilde{p}, v) = - \int_{\Omega \setminus A} (y - \bar{y})v \, dx \quad \forall v \in H_0^1(\Omega \setminus A) \quad (18)$$

with  $a_{\Omega \setminus A}$  being the restriction of the bilinear form  $a(\cdot, \cdot)$  to  $\Omega \setminus A$ . Further, the solutions  $p_c$  of eq. (16) converge strongly in  $H_0^1(\Omega)$  to the  $H_0^1$ -representation of  $p$ .

*Proof.* Let us consider the regularized problem (9) for  $\gamma, c > 0$ . Existence and uniqueness of solutions  $y_{\gamma,c}, p_{\gamma,c}$  of regularized state and adjoint are guaranteed by application of the Minty-Browder Theorem in analogy to theorem 1 for  $y_{\gamma,c}$  and the Lax-Milgram Theorem for  $p_{\gamma,c}$ , respectively.

This proof consists of two main parts:

1. Showing the  $H^1$ -convergence of the smoothed to the non-smoothed regularized adjoint  $p_{\gamma,c} \rightarrow p_c$  for  $\gamma \rightarrow \infty$ .
2. Analyzing the limit PDE (16) for  $c \rightarrow \infty$  and proving that  $p_c \rightarrow p$  in  $H^1(\Omega)$  for  $c \rightarrow \infty$ , where  $p$  is defined as in (17).

**To 1.** We start to show the  $H^1$ -convergence of the smoothed to the non-smoothed regularized adjoint  $p_{\gamma,c} \rightarrow p_c$  for  $\gamma \rightarrow \infty$ .

The assumption (15) of  $L^1$ -convergence of  $\text{sign}_\gamma(\bar{\lambda} + c \cdot (y_{\gamma,c} - \varphi))$  is equivalent to  $L^p$ -convergence for all  $p \in [1, \infty)$  in our setting, since

$$\begin{aligned} & \|\text{sign}_\gamma(\bar{\lambda} + c \cdot (y_{\gamma,c} - \varphi)) - \text{sign}(\bar{\lambda} + c \cdot (y_c - \varphi))\|_{L^p(\Omega)} \\ & \leq \|\text{sign}_\gamma(\bar{\lambda} + c \cdot (y_{\gamma,c} - \varphi)) - \text{sign}(\bar{\lambda} + c \cdot (y_c - \varphi))\|_{L^1(\Omega)}^{1/p} \\ & \leq \|\text{sign}_\gamma(\bar{\lambda} + c \cdot (y_{\gamma,c} - \varphi)) - \text{sign}(\bar{\lambda} + c \cdot (y_c - \varphi))\|_{L^1(\Omega)} \rightarrow 0 \quad \text{for } \gamma \rightarrow \infty. \end{aligned}$$

Denote by  $S_{\gamma,c}: H_0^1(\Omega) \rightarrow H^{-1}(\Omega)$  the linear operator corresponding to the left-hand side of the smoothed adjoint equation (10) and  $S_c: H^1(\Omega) \rightarrow H^{-1}(\Omega)$  the one to (16). We establish convergence of  $S_{\gamma,c}$  to  $S_c$  in the operator norm. In the following, we apply the Hölder's inequality and make use of the fact that  $L^q(\Omega)$  embeds into  $L^p(\Omega)$  for  $1 \leq p < q \leq \infty$  for finite measure spaces with a constant  $C$  for the embedding depending on  $p$  and  $q$ . Moreover, we use  $L^p$ -convergence of

$\text{sign}_\gamma(\bar{\lambda} + c \cdot (y_{\gamma,c} - \varphi))$  for all  $p \in [1, \infty)$  as well as boundedness of  $\text{sign}_\gamma$  and  $\text{sign}$ . All this yields

$$\begin{aligned}
& \|S_{\gamma,c} - S_c\|_{\text{op}} \\
&= \sup_{\substack{g \in H_0^1(\Omega) \\ \|g\|=1}} \sup_{\substack{h \in H_0^1(\Omega) \\ \|h\|=1}} c \cdot |((\text{sign}_\gamma(\bar{\lambda} + c \cdot (y_{\gamma,c} - \varphi)) - \text{sign}(\bar{\lambda} + c \cdot (y_c - \varphi))) \cdot g, h)_{L^2(\Omega)}| \\
&\leq \sup_{\substack{g \in H_0^1(\Omega) \\ \|g\|=1}} \sup_{\substack{h \in H_0^1(\Omega) \\ \|h\|=1}} c \cdot \|(\text{sign}_\gamma(\bar{\lambda} + c \cdot (y_{\gamma,c} - \varphi)) \\
&\quad - \text{sign}(\bar{\lambda} + c \cdot (y_c - \varphi))) \cdot g\|_{L^2(\Omega)} \cdot \|h\|_{L^2(\Omega)} \\
&\leq \sup_{\substack{g \in H_0^1(\Omega) \\ \|g\|=1}} \sup_{\substack{h \in H_0^1(\Omega) \\ \|h\|=1}} C \cdot c \cdot \|(\text{sign}_\gamma(\bar{\lambda} + c \cdot (y_{\gamma,c} - \varphi)) \\
&\quad - \text{sign}(\bar{\lambda} + c \cdot (y_c - \varphi))) \cdot g\|_{L^1(\Omega)} \cdot \|h\|_{L^2(\Omega)} \\
&\leq C \cdot c \cdot \|\text{sign}_\gamma(\bar{\lambda} + c \cdot (y_{\gamma,c} - \varphi)) - \text{sign}(\bar{\lambda} + c \cdot (y_c - \varphi))\|_{L^2(\Omega)} \rightarrow 0 \quad \text{for } \gamma \rightarrow \infty,
\end{aligned}$$

which gives the desired convergence in the operator norm. Using analyticity of the inversion  $\mathcal{I}: S \mapsto S^{-1}$  in the domain of invertible, bounded, linear operators given in our setting, convergence of the solution operators  $S_{\gamma,c}^{-1} \rightarrow S_c^{-1}$  in operator norm is implied immediately, see e.g., [44, page 237]. Combining this with the convergence of  $y_{\gamma,c} \rightarrow y_c$  in  $H_0^1(\Omega)$  established by theorem 1 yields

$$\begin{aligned}
& \|p_{\gamma,c} - p_c\|_{H_0^1(\Omega)} \\
&= \| -S_{\gamma,c}^{-1}(y_{\gamma,c} - \bar{y}) + S_c^{-1}(y_c - \bar{y}) \|_{H_0^1(\Omega)} \\
&\leq \|S_{\gamma,c}^{-1}(y_{\gamma,c} - \bar{y}) - S_{\gamma,c}^{-1}(y_c - \bar{y})\|_{H_0^1(\Omega)} + \|S_{\gamma,c}^{-1}(y_c - \bar{y}) - S_c^{-1}(y_c - \bar{y})\|_{H_0^1(\Omega)} \\
&\leq \|S_{\gamma,c}^{-1}\|_{\text{op}} \|y_{\gamma,c} - y_c\|_{H_0^1(\Omega)} + \|S_{\gamma,c}^{-1} - S_c^{-1}\|_{\text{op}} \|y_c - \bar{y}\|_{H_0^1(\Omega)} \rightarrow 0 \quad \text{for } \gamma \rightarrow \infty,
\end{aligned}$$

since  $\|S_{\gamma,c}^{-1}\|_{\text{op}}$  can be bounded due to convergence.

**To 2.** Next, we analyze the limit PDE (16) for  $c \rightarrow \infty$ . We show that  $p_c \rightarrow p$  in  $H^1(\Omega)$  for  $c \rightarrow \infty$ , where  $p$  is defined as in (17). For this, we first notice that our assumption concerning regular decomposability of  $A = \{x \in \Omega \mid y - \varphi \geq 0\}$  ensures that  $\partial A = \{x \in \Omega \mid y - \varphi = 0\}$  forms a  $C^{0,1}$ -submanifold of  $\Omega$ . This in turn leads to the well-posedness of the variational problem (18) and, thus, of  $p \in H_0^1(\Omega)$ . Our next step is to show

$$p_c \rightarrow p \quad \text{in } H^1(\Omega) \text{ for } c \rightarrow \infty. \quad (19)$$

To show this, we artificially constrain problem (16) to  $A \subseteq \Omega$ . So denote by  $a_A(\cdot, \cdot)$  the restriction of the bilinear form  $a(\cdot, \cdot)$  to  $A \subseteq \Omega$ . The corresponding restricted problem becomes

$$a_A(p_{c|_A}, v) + c \cdot \int_A \mathbb{1}_{A_c} \cdot p_{c|_A} \cdot v \, dx = - \int_A (y_c - \bar{y}) \cdot v \, dx \quad \forall v \in H_0^1(A), \quad (20)$$

where the Dirichlet condition  $p_{c|_A} = p_c$  on  $\partial A$  is incorporated in the usual way. Dividing by  $c > 0$  gives an equivalent equation in the sense that a solution  $p_{c|_A} \in H^1(A)$  to eq. (20) also solves the equivalent equation

$$\frac{1}{c} \cdot a_A(p_{c|_A}, v) + \int_A \mathbb{1}_{A_c} \cdot p_{c|_A} \cdot v \, dx = - \frac{1}{c} \cdot \int_A (y_c - \bar{y}) \cdot v \, dx \quad \forall v \in H_0^1(A). \quad (21)$$

The differential operator corresponding to the left-hand side of the equivalent equation is given by (21):

$$S_{A,c}: H^1(A) \rightarrow H^{-1}(A), \quad p \mapsto \frac{1}{c} \cdot a_A(p, \cdot) + (\mathbb{1}_{A_c} \cdot p, \cdot)_{L^2(A)}. \quad (22)$$

Next, we show that the differential operators  $S_{A,c}$  converge in the linear operator norm  $\|\cdot\|_{\text{op}}$  with the limit operator

$$S_A: H^1(A) \rightarrow H^{-1}(A), p \mapsto (p, \cdot)_{L^2(A)}. \quad (23)$$

This is clear, since

$$\begin{aligned} & \|S_{A,c} - S_A\|_{\text{op}} \\ &= \sup_{\substack{g \in H_0^1(A) \\ \|g\|=1}} \sup_{\substack{h \in H_0^1(A) \\ \|h\|=1}} \left| \frac{1}{c} \cdot a_A(g, h) - \int_{A \setminus A_c} g \cdot h \, dx \right| \\ &\leq \sup_{\substack{g \in H_0^1(A) \\ \|g\|=1}} \sup_{\substack{h \in H_0^1(A) \\ \|h\|=1}} \left( \frac{1}{c} \left( \sum_{i,j} \|a_{i,j}\|_{L^\infty(\Omega)} + \sum_j \|d_j\|_{L^\infty(\Omega)} + \|b\|_{L^\infty(\Omega)} \right) \right. \\ &\quad \cdot \|g\|_{H_0^1(A)} \cdot \|h\|_{H_0^1(A)} \\ &\quad \left. + C \cdot \text{vol}(A \setminus A_c) \cdot \|g\|_{H_0^1(A)} \cdot \|h\|_{H_0^1(A)} \right) \\ &= \frac{1}{c} \left( \sum_{i,j} \|a_{i,j}\|_{L^\infty(\Omega)} + \sum_j \|d_j\|_{L^\infty(\Omega)} + \|b\|_{L^\infty(\Omega)} \right) + C \cdot \text{vol}(A \setminus A_c) \\ &\rightarrow 0 \quad \text{for } c \rightarrow \infty, \end{aligned}$$

since  $\text{vol}(A \setminus A_c) \rightarrow 0$  for  $c \rightarrow \infty$ , which would otherwise contradict  $y_c \rightarrow y$  in  $H_0^1(\Omega)$ . We can now apply a similar argument as in Step 1, namely the analyticity of the inversion operator  $\mathcal{I}: S \mapsto S^{-1}$ , giving us convergence of the solution operators  $S_{A,c}^{-1} \rightarrow S_A^{-1}$  in  $\|\cdot\|_{\text{op}}$ . Also notice that we can obtain the sequence of solutions  $p_{c|A}$  by solving eq. (21) with the corresponding right hand sides  $-\frac{1}{c}(y_c - \bar{y})$  instead of the original equation (20) and that the right hand sides converge to 0 in  $H^1(\Omega)$  as  $c \rightarrow \infty$ . We conclude

$$\begin{aligned} 0 &\leq \|p_c\|_{H^1(A)} = \|S_{A,c}^{-1} \left( -\frac{1}{c}(y_c - \bar{y}) \right)\|_{H^1(A)} \\ &\leq \frac{1}{c} \|(S_{A,c}^{-1} - S_A^{-1})(y_c - \bar{y})\|_{H^1(A)} + \frac{1}{c} \|S_A^{-1}(y_c - \bar{y})\|_{H^1(A)} \\ &\leq \frac{1}{c} (\|S_{A,c}^{-1} - S_A^{-1}\|_{\text{op}} + \|S_A^{-1}\|_{\text{op}}) \cdot (\|y_c - y\|_{H^1(A)} + \|\bar{y}\|_{H^1(A)}) \\ &\rightarrow 0 \quad \text{for } c \rightarrow \infty. \end{aligned}$$

For the proof of convergence it remains to address the convergence of  $p_c$  on  $\Omega \setminus A$ . We can artificially restrict eq. (16) to  $\Omega \setminus A$  by imposing the Dirichlet boundary  $p_{c|A}$  on  $\partial A$ , since  $\partial A$  forms a  $C^{0,1}$ -submanifold of  $\Omega$  as we assumed regular decomposability (cf. definition 1) of the active set  $A$ . To distinguish the corresponding bilinear forms, we denote the restricted bilinear form by  $a_{\Omega \setminus A}$ . Since the unrestricted bilinear form  $a(\cdot, \cdot)$  is elliptic, coercivity for some constant  $K > 0$  also holds for  $a_{\Omega \setminus A}$ . This together with Hölders inequality, assumption  $A_c \subseteq A$  for all  $c > 0$  and the fact that  $p_c - \tilde{p} \in H_0^1(\Omega \setminus A)$  can act as a testfunction gives

$$\begin{aligned} 0 &\leq K \|p_c - \tilde{p}\|_{H^1(\Omega \setminus A)}^2 \leq a_{\Omega \setminus A}(p_c - \tilde{p}, p_c - \tilde{p}) = a_{\Omega \setminus A}(p_c, p_c - \tilde{p}) - a_{\Omega \setminus A}(\tilde{p}, p_c - \tilde{p}) \\ &= -c \int_{\Omega \setminus A} \mathbb{1}_{A_c} p_c (p_c - \tilde{p}) \, dx - \int_{\Omega \setminus A} (y_c - \bar{y})(p_c - \tilde{p}) \, dx + \int_{\Omega \setminus A} (y - \bar{y})(p_c - \tilde{p}) \, dx \\ &= \int_{\Omega \setminus A} (y - y_c)(p_c - \tilde{p}) \, dx \leq \|y_c - y\|_{H^1(\Omega)} \|p_c - \tilde{p}\|_{H^1(\Omega \setminus A)}, \end{aligned}$$

where  $\tilde{p} \in H^1(\Omega \setminus A)$  is defined as in (18). This results in

$$p_c \rightarrow p \quad \text{in } H_0^1(\Omega \setminus A) \quad \text{for } c \rightarrow \infty \quad (24)$$

due to our assumptions and  $y_c \rightarrow y$  in  $H^1(\Omega)$  as by proposition 1. Together with eq. (19) this gives the desired convergence  $p_c \rightarrow p$  in  $H_0^1(\Omega)$ .  $\square$

There are a few non-trivial assumptions in theorem 1: assumption (iv) and (v). In the following, we formulate two remarks in which we address these assumptions (cf. remark 3 for (iv) and remark 4 for (v)).

**Remark 3.** *It is possible to fulfill assumption (14) on inclusion of the active sets  $A_c \subset A$  by choosing a sufficient  $\bar{\lambda} \in L^2(\Omega)$ . To be more precisely, since we assume  $\varphi \in H^2(\Omega)$ , we can choose  $\bar{\lambda} := \max\{0, f - S\varphi\}$  with  $S$  being the differential operator corresponding to the elliptic bilinear form  $a(\cdot, \cdot)$  in (5), guaranteeing feasibility  $y_{c_1} \leq y_{c_2} \leq y \leq \varphi$  for all  $0 < c_1 \leq c_2$ . For the proof of this, we refer to [22, Section 3.2].*

**Remark 4.** *Assumption 15 ensures that convergence of  $\text{sign}_\gamma$  is compatible with convergence of  $y_{\gamma,c}$  for  $\gamma \rightarrow \infty$ . For giving a working example, we verify this assumption in the numerical section under eq. (45) for several demonstrative cases.*

**Remark 5.** *The limit object  $p \in H_0^1(\Omega)$  of the adjoints  $p_{\gamma,c}$  as defined in (17) is the solution of an elliptic problem (18) on a domain  $\Omega \setminus A$  with topological dimension greater than 0. This can be exploited in numerical computations, for instance by a fat boundary method for finite elements on domains with holes as proposed by the authors of [30].*

## 3.2 Shape derivatives

In this section, we apply our convergence results for the regularized state and adjoint equations to derive similar convergence results for the shape derivatives of the shape optimization problem constrained by the fully regularized state equation (9). In general, shape derivatives of the unregularized VI constrained shape optimization problems do not exist (cf., e.g., [38, Chapter 1.1]). Nevertheless, we show existence of an object behaving as a shape derivative as well as convergence of the shape derivatives of the fully regularized problem to the latter. In the following, we split the main results into two theorems, the first one being the shape derivative for the fully regularized equation, the second one being convergence of the former for  $\gamma, c \rightarrow \infty$ .

The shape derivative of a general shape functional  $H$  at  $\Omega$  in direction of a sufficiently smooth vector field  $V$  is denoted by  $DH(\Omega)[V]$ . For the definition of shape derivatives or a detailed introduction into shape calculus, we refer to the monographs [11, 38]. In general, we have to deal with so-called material and shape derivatives of generic functions  $h: \Omega \rightarrow \mathbb{R}$  in order to derive shape derivatives of objective shape functions. For their definitions and more details we refer to the literature, e.g., [34]. In the following, we denote the material derivative of  $h$  by  $\dot{h}$  or  $D_m(h)$  and the shape derivative of  $h$  in the direction of a vector field  $V$  is denoted by  $h'$ .

**Remark 6.** *In this section, we only consider the shape functional  $J$  defined in (1) without regularization term  $\mathcal{J}_{\text{reg}}$ , i.e., we focus only on  $\mathcal{J}$ . The shape derivative of  $J$  is given by the sum of the shape derivative of  $\mathcal{J}$  and  $\mathcal{J}_{\text{reg}}$ , where  $D\mathcal{J}_{\text{reg}}(\Omega)[V] = \nu \int_{\Gamma_{\text{int}}} \kappa(V, n) ds$  with  $\kappa := \text{div}_{\Gamma_{\text{int}}}(n)$  denoting the mean curvature of  $\Gamma_{\text{int}}$ . Please note that the objective functional and the shape derivative in correlation with the regularized VI (9) depends on the parameters  $\gamma$  and  $c$ . In order to denote this dependency, we use the notation  $\mathcal{J}_{\gamma,c}$  and  $D\mathcal{J}_{\gamma,c}(\Omega)[V]$  for the objective functional and its shape derivative, respectively.*

We state the first theorem, which presents the shape derivative of the objective functional  $\mathcal{J}$  defined in (1) constrained by the fully regularized VI (9).

**Theorem 2.** *Assume the setting of the shape optimization problem formulated in section 2. Let the assumptions of theorem 1 hold. Moreover, let  $M := (a_{i,j})_{i,j=1,2}$  be the matrix of coefficient functions to the leading order terms in (4). Furthermore, assume  $D_m(y_{\gamma,c}), D_m(p_{\gamma,c}) \in H_0^1(\Omega)$  for all  $\gamma, c > 0$ . Then the shape derivatives of  $\mathcal{J}$  defined in (1) constrained by a fully regularized VI (9) in direction of a vector field  $V \in H_0^1(\Omega)$  exist and are given by*

$$\begin{aligned}
& D\mathcal{J}_{\gamma,c}(\Omega)[V] \\
&= \int_{\Omega} -(y_{\gamma,c} - \bar{y})\nabla\bar{y}^T V - \nabla y_{\gamma,c}^T (\nabla V^T M - \nabla M \cdot V + M^T \nabla V) \nabla p_{\gamma,c} \\
&\quad + (\nabla b^T V) y_{\gamma,c} p_{\gamma,c} + y_{\gamma,c} \cdot ((\nabla d^T V)^T \nabla p_{\gamma,c} - d^T (\nabla V \nabla p_{\gamma,c})) \\
&\quad + p_{\gamma,c} \cdot ((\nabla d^T V)^T \nabla y_{\gamma,c} - d^T (\nabla V \nabla y_{\gamma,c})) \\
&\quad + \text{sign}_{\gamma}(\bar{\lambda} + c \cdot (y_{\gamma,c} - \varphi)) \cdot (\nabla \bar{\lambda} - c \cdot \nabla \varphi)^T V \cdot p_{\gamma,c} - \nabla f^T V p_{\gamma,c} \quad (25) \\
&\quad + \text{div}(V) \left( \frac{1}{2} (y_{\gamma,c} - \bar{y})^2 + b y_{\gamma,c} p_{\gamma,c} + \sum_{i,j} a_{i,j} \partial_i y_{\gamma,c} \partial_j p_{\gamma,c} \right. \\
&\quad \quad \left. + \sum_i d_i (\partial_i y_{\gamma,c} p_{\gamma,c} + y_{\gamma,c} \partial_i p_{\gamma,c}) \right. \\
&\quad \quad \left. + \max_{\gamma}(\bar{\lambda} + c \cdot (y_{\gamma,c} - \varphi)) p_{\gamma,c} - f p_{\gamma,c} \right) dx.
\end{aligned}$$

*Proof.* Let us consider the shape optimization problem with fully regularized state equations with parameters  $\gamma, c > 0$  as in (9) and fixed shape  $\Gamma_{\text{int}}$  to derive corresponding shape derivative. By definition it's Lagrangian function is given by

$$\begin{aligned}
\mathcal{L}_{\gamma,c}(y_{\gamma,c}, p_{\gamma,c}, \Omega) &= \frac{1}{2} \int_{\Omega} (y_{\gamma,c} - \bar{y})^2 dx + a(y_{\gamma,c}, p_{\gamma,c}) \\
&\quad + (\max_{\gamma}(\bar{\lambda} + c \cdot (y_{\gamma,c} - \varphi)), p_{\gamma,c})_{L^2(\Omega)} - (f, p_{\gamma,c})_{L^2(\Omega)}
\end{aligned} \quad (26)$$

First, we show the existence of the shape derivatives by the min-max formulation of Correa and Seeger.<sup>1</sup> Since for all  $y_{\gamma,c} \in H_0^1(\Omega)$

$$\sup_{y_{\gamma,c} \in H_0^1(\Omega)} \mathcal{L}_{\gamma,c}(y_{\gamma,c}, p_{\gamma,c}, \Omega) = \begin{cases} \mathcal{J}_{\gamma,c}(\Omega) & \text{if } y_{\gamma,c} \text{ solves (9)} \\ \infty & \text{else} \end{cases},$$

we get

$$\mathcal{J}_{\gamma,c}(\Omega) = \min_{y_{\gamma,c} \in H_0^1(\Omega)} \sup_{p_{\gamma,c} \in H_0^1(\Omega)} \mathcal{L}_{\gamma,c}(y_{\gamma,c}, p_{\gamma,c}, \Omega). \quad (27)$$

In order to apply the theorem of Correa and Seeger [8, theorem 2.1] to the Lagrangian, we have to show that it admits saddle points.

The following argumentation is in analogy to [24, Section 4.2]. By the assumption 1 (iii), which states that  $\text{sign}_{\gamma}$  is nondecreasing, we have convexity of  $\max_{\gamma}: \mathbb{R} \rightarrow \mathbb{R}$  as a real function. This in turn gives us convexity of the monotone Nemetskii-operator  $\Phi_{\gamma}$  defined in (13). Thus, the Lagrangian  $\mathcal{L}_{\gamma,c}$  is convex in the state  $y_{\gamma,c} \in H_0^1(\Omega)$ . Furthermore, differentiability of  $\mathcal{L}_{\gamma,c}$  with respect to  $y_{\gamma,c}$  and  $p_{\gamma,c}$  as well as concavity in the adjoint argument  $p_{\gamma,c} \in H_0^1(\Omega)$  can be verified easily. Therefore, by [40, Proposition 1.6, p. 169170], the saddle points described in (27)

<sup>1</sup>Please note that there are various approaches to show the shape differentiability of a shape functional: the material and shape derivative method, the min-max formulation of Correa and Seeger and the rearrangement method. We refer to [39] for alternative approaches.

are characterized by (9) and (10). Since (9) and (10) admit unique solutions, as by argumentation in the proof of theorem 1, we indeed have unique saddle points characterized by the state solutions  $y_{\gamma,c}$  and adjoints solutions  $p_{\gamma,c}$  for given parameters  $\gamma, c > 0$ . Following the argumentation in [24, Section 4.2, p. 288ff], we get existence of shape derivatives  $D\mathcal{J}_{\gamma,c}$  for all  $\gamma, c > 0$ .

Next, we derive the shape derivative expression. By applying standard shape calculus techniques (cf. [3, 42]) to the target functional part of the Lagrangian we get

$$\begin{aligned} & D\left(\frac{1}{2}\int_{\Omega}(y_{\gamma,c}-\bar{y})^2dx\right)[V] \\ &= \int_{\Omega}(y_{\gamma,c}-\bar{y})(D_m(y_{\gamma,c})-D_m(\bar{y})) + \operatorname{div}(V)(y_{\gamma,c}-\bar{y})^2dx \\ &= \int_{\Omega}(y_{\gamma,c}-\bar{y})D_m(y_{\gamma,c})dx + \int_{\Omega}-(y_{\gamma,c}-\bar{y})\nabla\bar{y}^TV + \operatorname{div}(y_{\gamma,c}-\bar{y})^2dx, \end{aligned} \quad (28)$$

since the target  $\bar{y} \in L^2(\Omega)$  does not depend on the shape. Next, as similarly found in, e.g., [42], we calculate the shape derivative of the bilinear form  $a(\cdot, \cdot)$ . For avoiding confusion with the active sets  $A$  and  $A_c$ , we call the coefficient matrix  $(a_{i,j})_{i,j}$  of the leading order parts of the bilinear form  $M$ . As before we have

$$\begin{aligned} D(a(y_{\gamma,c}, p_{\gamma,c}))[V] &= \int_{\Omega} D_m(a(y_{\gamma,c}, p_{\gamma,c})) + \operatorname{div}(V)\left(\sum_{i,j} a_{i,j}\partial_i y_{\gamma,c}\partial_j p_{\gamma,c}\right. \\ &\quad \left.+ \sum_i d_i(\partial_i y_{\gamma,c}p_{\gamma,c} + y_{\gamma,c}\partial_i p_{\gamma,c}) + by_{\gamma,c}p_{\gamma,c}\right)dx. \end{aligned} \quad (29)$$

We use linearity, chain rules, product rules and gradient identities for the material derivative  $D_m(\cdot)$ , as found in [3], to reformulate  $D_m(a(y_{\gamma,c}, p_{\gamma,c}))$ . For readability, we analyze each term individually. We start with the leading order terms:

$$\begin{aligned} & D_m\left(\sum_{i,j} a_{i,j}\partial_i y_{\gamma,c}\partial_j p_{\gamma,c}\right) \\ &= \sum_{i,j} D_m(a_{i,j})\partial_i y_{\gamma,c}\partial_j p_{\gamma,c} + a_{i,j}D_m(\partial_i y_{\gamma,c})\partial_j p_{\gamma,c} + a_{i,j}\partial_i y_{\gamma,c}D_m(\partial_j p_{\gamma,c}) \\ &= \sum_{i,j} D_m(a_{i,j})\partial_i y_{\gamma,c}\partial_j p_{\gamma,c} + a_{i,j}\left((\partial_i D_m(y_{\gamma,c}) - \sum_k \partial_k y_{\gamma,c}\partial_i V_k)\partial_j p_{\gamma,c}\right. \\ &\quad \left.+ \partial_i y_{\gamma,c}(\partial_j D_m(p_{\gamma,c}) - \sum_k \partial_k p_{\gamma,c}\partial_j V_k)\right) \\ &= \sum_{i,j} \left(\nabla a_{i,j}^T V \partial_i y_{\gamma,c} \partial_j p_{\gamma,c} + a_{i,j} \partial_i D_m(y_{\gamma,c}) \partial_j p_{\gamma,c} + a_{i,j} \partial_i y_{\gamma,c} \partial_j D_m(p_{\gamma,c})\right. \\ &\quad \left.- a_{i,j}(\partial_i V^T \nabla y_{\gamma,c}) \partial_j p_{\gamma,c} - a_{i,j} \partial_i y_{\gamma,c} (\partial_j V^T \nabla p_{\gamma,c})\right) \\ &= \nabla y_{\gamma,c}^T (\nabla M^T V) \nabla p_{\gamma,c} + \sum_{i,j} \left(a_{i,j} \partial_i D_m(y_{\gamma,c}) \partial_j p_{\gamma,c} + a_{i,j} \partial_i y_{\gamma,c} \partial_j D_m(p_{\gamma,c})\right) \\ &\quad - \nabla y_{\gamma,c}^T (\nabla V^T M) \nabla p_{\gamma,c} - \nabla y_{\gamma,c}^T (M \nabla V) \nabla p_{\gamma,c} \end{aligned}$$

For the first order terms of  $a(\cdot, \cdot)$  we only compute  $y_{\gamma,c} d^T \nabla p_{\gamma,c}$ , since calculations

are analogous for the second term by switching the roles of  $y_{\gamma,c}$  and  $p_{\gamma,c}$ . We get

$$\begin{aligned}
& D_m(y_{\gamma,c} d^T \nabla p_{\gamma,c}) \\
&= D_m(y_{\gamma,c}) d^T \nabla p_{\gamma,c} + y_{\gamma,c} \cdot \sum_i (D_m(d_i) \partial_i p_{\gamma,c} + d_i D_m(\partial_i p_{\gamma,c})) \\
&= D_m(y_{\gamma,c}) d^T \nabla p_{\gamma,c} \\
&\quad + \sum_i \left( y_{\gamma,c} (\nabla d_i^T V) \partial_i p_{\gamma,c} + y_{\gamma,c} d_i \partial_i D_m(p_{\gamma,c}) - \sum_k (y_{\gamma,c} d_i \partial_k p_{\gamma,c} \partial_i V_k) \right) \\
&= D_m(y_{\gamma,c}) d^T \nabla p_{\gamma,c} + y_{\gamma,c} (\nabla d^T V)^T \nabla p_{\gamma,c} + y_{\gamma,c} d^T \nabla D_m(p_{\gamma,c}) - y_{\gamma,c} d^T (\nabla V \nabla p),
\end{aligned}$$

where we again use shape independence of the coefficient functions of  $a(\cdot, \cdot)$ . For the term of order zero we apply the product rule for material derivatives and shape independence of coefficient functions:

$$D_m(b y_{\gamma,c} p_{\gamma,c}) = (\nabla b^T V) y_{\gamma,c} p_{\gamma,c} + b D_m(y_{\gamma,c}) p_{\gamma,c} + b y_{\gamma,c} D_m(p_{\gamma,c})$$

Combining these formulas, plugging them into eq. (28) and collecting all material derivatives of  $y_{\gamma,c}$  and  $p_{\gamma,c}$  result in the shape derivative of the bilinear form  $a(\cdot, \cdot)$ :

$$\begin{aligned}
& D\left(a(y_{\gamma,c}, p_{\gamma,c})\right)[V] \\
&= a(D_m(y_{\gamma,c}), p_{\gamma,c}) + a(y_{\gamma,c}, D_m(p_{\gamma,c})) \\
&\quad + \int_{\Omega} \nabla y_{\gamma,c}^T (\nabla M^T V - \nabla V^T N - M \nabla V) \nabla p_{\gamma,c} \\
&\quad + y_{\gamma,c} \cdot ((\nabla d^T V)^T \nabla p_{\gamma,c} - d^T (\nabla V \nabla p_{\gamma,c})) \\
&\quad + p_{\gamma,c} \cdot ((\nabla d^T V)^T \nabla y_{\gamma,c} - d^T (\nabla V \nabla y_{\gamma,c})) + (\nabla b^T V) y_{\gamma,c} p_{\gamma,c} \\
&\quad + \operatorname{div}(V) \left( \sum_{i,j} a_{i,j} \partial_i y_{\gamma,c} \partial_j p_{\gamma,c} + \sum_i d_i (\partial_i y_{\gamma,c} p_{\gamma,c} + y_{\gamma,c} \partial_i p_{\gamma,c}) + b y_{\gamma,c} p_{\gamma,c} \right) dx
\end{aligned}$$

The shape derivative of the term including  $\max_{\gamma}$  is calculated by chain rule, which is applicable since we assume sufficient smoothness of  $\max_{\gamma}$ :

$$\begin{aligned}
& D\left((\max_{\gamma}(\bar{\lambda} + c \cdot (y_{\gamma,c} - \varphi)), p_{\gamma,c})_{L^2(\Omega)}\right)[V] \\
&= \int_{\Omega} D_m\left((\max_{\gamma}(\bar{\lambda} + c \cdot (y_{\gamma,c} - \varphi)), p_{\gamma,c})_{L^2(\Omega)}\right) \\
&\quad + \operatorname{div}(V) \max_{\gamma}(\bar{\lambda} + c \cdot (y_{\gamma,c} - \varphi)) p_{\gamma,c} dx
\end{aligned}$$

with

$$\begin{aligned}
& D_m\left((\max_{\gamma}(\bar{\lambda} + c \cdot (y_{\gamma,c} - \varphi)), p_{\gamma,c})_{L^2(\Omega)}\right) \\
&= (\operatorname{sign}_{\gamma}(\bar{\lambda} + c \cdot (y_{\gamma,c} - \varphi)) D_m(\bar{\lambda} + c \cdot (y_{\gamma,c} - \varphi)), p_{\gamma,c})_{L^2(\Omega)} \\
&\quad + (\max_{\gamma}(\bar{\lambda} + c \cdot (y_{\gamma,c} - \varphi)), D_m(p_{\gamma,c}))_{L^2(\Omega)} \\
&= (\operatorname{sign}_{\gamma}(\bar{\lambda} + c \cdot (y_{\gamma,c} - \varphi)) (\nabla \bar{\lambda} - c \nabla \varphi)^T V, p_{\gamma,c})_{L^2(\Omega)} \\
&\quad + (c \cdot \operatorname{sign}_{\gamma}(\bar{\lambda} + c \cdot (y_{\gamma,c} - \varphi)) p_{\gamma,c}, D_m(y_{\gamma,c}))_{L^2(\Omega)} \\
&\quad + (\max_{\gamma}(\bar{\lambda} + c \cdot (y_{\gamma,c} - \varphi)), D_m(p_{\gamma,c}))_{L^2(\Omega)}
\end{aligned}$$

The shape derivative of the last term in the Lagrangian (26) is given by a simple product rule

$$D((f, p_{\gamma,c})_{L^2(\Omega)})[V] = (D_m(f), p_{\gamma,c})_{L^2(\Omega)} + (f, D_m(p_{\gamma,c}))_{L^2(\Omega)}.$$

Since we can apply a regularity theorem for elliptic PDE (cf. [13, p. 317, theorem 4]) due to our assumption on the coefficients of  $a(\cdot, \cdot)$  and  $c \cdot \text{sign}(\bar{\lambda} + c \cdot (y_{\gamma,c} - \varphi)) \in L^\infty(\Omega)$  acting as a coefficient function, we get  $p_{\gamma,c} \in H_0^2(\Omega)$  and, thus,  $D_m(p_{\gamma,c}) \in H_0^1(\Omega)$ . We now use the assumptions  $D_m(y_{\gamma,c}), D_m(p_{\gamma,c}) \in H_0^1(\Omega)$ . If we rearrange the terms with  $D_m(y_{\gamma,c})$  and  $D_m(p_{\gamma,c})$  acting as test functions and applying the saddle point conditions, which means that the state equation (9) and adjoint equation (10) are fulfilled, the terms consisting  $D_m(y_{\gamma,c})$  and  $D_m(p_{\gamma,c})$  cancel. By adding all terms of eq. (26), the shape derivative  $D\mathcal{J}_{\gamma,c}(\Omega)[V]$  as in (25) is established.  $\square$

**Remark 7.** *One can fulfill the assumptions of the theorem of Correa and Seeger and, thus, guarantee the existence of the shape derivative without a computation of the material derivatives  $D_m(y_{\gamma,c}), D_m(p_{\gamma,c})$ . The assumption  $D_m(y_{\gamma,c}), D_m(p_{\gamma,c}) \in H_0^1(\Omega)$  for all  $\gamma, c > 0$  in theorem 2 is only needed in order to calculate the shape derivative expression (25).*

**Remark 8.** *The assumption  $D_m(y_{\gamma,c}) \in H_0^1(\Omega)$  in theorem 2 is needed to apply the saddle point conditions. For this, it is sufficient that  $y_{\gamma,c} \in H_0^2(\Omega)$ . For example, this regularity can be ensured by additionally assuming  $d \equiv 0, b \equiv 0$  for the coefficients of the elliptic bilinear form  $a(\cdot, \cdot)$  together with  $\varphi > 0$  and choosing  $\bar{\lambda} \in L^\infty(\Omega)$ . The latter two assumptions imply that the maximal monotone Nemetskii-operator (13) is equal to 0 for  $y_{\gamma,c} = 0$  and sufficiently large  $\gamma, c > 0$ . In combination with the former assumptions, [4, Theorem A.1.] can be applied to get  $y_{\gamma,c} \in H_0^2(\Omega)$  for all sufficiently large  $\gamma, c > 0$ .*

**Remark 9.** *The assumption  $D_m(p_{\gamma,c}) \in H_0^1(\Omega)$  in theorem 2 can be fulfilled, e.g., by assuming additional regularity  $a_{i,j} \in C^1(\bar{\Omega})$  of the leading coefficients of the bilinear form  $a(\cdot, \cdot)$  and  $C^2$ -regularity of the boundary  $\partial\Omega$ . This together with the fact that  $c \cdot \text{sign}_\gamma(\bar{\lambda} + c \cdot (y_{\gamma,c} - \varphi)) \in L^\infty(\Omega)$  acts as part of the coefficient function of the zero order terms permit application of a regularity theorem for linear elliptic problems (cf. [13, p. 317, theorem 4]) giving  $p_{\gamma,c} \in H^2(\Omega)$ . This in turn guarantees  $D_m(p_{\gamma,c}) \in H_0^1(\Omega)$ .*

Next, we formulate the second main theorem of this section, which states the convergence of the shape derivatives of the fully regularized problem.

**Theorem 3.** *Assume the setting of the shape optimization problem formulated in (2) and let the assumptions of theorem 1 hold. Moreover, let  $M := (a_{i,j})_{i,j=1,2}$  be the matrix of coefficient functions to the leading order terms in (4). Then, for all  $V \in H_0^1(\Omega)$ , the shape derivatives  $D\mathcal{J}_{\gamma,c}(\Omega)[V]$  in (25) converge to  $D\mathcal{J}(\Omega)[V]$  for  $\gamma, c \rightarrow \infty$ , where*

$$\begin{aligned}
& D\mathcal{J}(\Omega)[V] \\
& := \int_{\Omega} - (y - \bar{y}) \nabla \bar{y}^T V - \nabla y^T (\nabla V^T M - \nabla M \cdot V + M^T \nabla V) \nabla p \\
& \quad + y \cdot ((\nabla d^T V)^T \nabla p - d^T (\nabla V \nabla p)) + p \cdot ((\nabla d^T V)^T \nabla y - d^T (\nabla V \nabla y)) \\
& \quad + (\nabla b^T V) y p - \nabla f^T V p \\
& \quad + \text{div}(V) \left( \frac{1}{2} (y_{\gamma,c} - \bar{y})^2 + \sum_{i,j} a_{i,j} \partial_i y \partial_j p \right. \\
& \quad \left. + \sum_i d_i (\partial_i y p + y \partial_i p) + b y p - f p \right) dx \\
& \quad + \int_A (\varphi - \bar{y}) \nabla \varphi^T V dx.
\end{aligned} \tag{30}$$

*Proof.* We see that (25) already resembles (30) except for the three terms

$$T_0(V) := \int_{\Omega} \text{sign}_{\gamma}(\bar{\lambda} + c \cdot (y_{\gamma,c} - \varphi)) \cdot \nabla \bar{\lambda}^T V \cdot p_{\gamma,c} \, dx, \quad (31)$$

$$T_1(V) := -c \cdot \int_{\Omega} \text{sign}_{\gamma}(\bar{\lambda} + c \cdot (y_{\gamma,c} - \varphi)) \cdot \nabla \varphi^T V \cdot p_{\gamma,c} \, dx \quad (32)$$

$$T_2(V) := \int_{\Omega} \text{div}(V) \cdot \max_{\gamma}(\bar{\lambda} + c \cdot (y_{\gamma,c} - \varphi)) \cdot p_{\gamma,c} \, dx. \quad (33)$$

So showing convergence of  $D\mathcal{J}_{\gamma,c}$  is equivalent to showing convergence of the functionals  $T_0, T_1, T_2 : H_0^1(\Omega) \rightarrow \mathbb{R}$ , since all the other terms in (25) converge as  $p_{\gamma,c} \rightarrow p$  and  $y_{\gamma,c} \rightarrow y$  in  $H_0^1(\Omega)$  for  $\gamma, c \rightarrow \infty$  due to proposition 1 and theorem 1. First, we handle convergence of  $T_0$  for  $V \in H_0^1(\Omega)$ . Notice that

$$\begin{aligned} & \int_{\Omega} \text{sign}_{\gamma}(\bar{\lambda} + c \cdot (y_{\gamma,c} - \varphi)) \cdot \nabla \bar{\lambda}^T V \cdot p_{\gamma,c} \, dx \\ & \rightarrow \int_{\Omega} \text{sign}(\bar{\lambda} + c \cdot (y_c - \varphi)) \cdot \nabla \bar{\lambda}^T V \cdot p_c \, dx \end{aligned} \quad (34)$$

for  $\gamma \rightarrow \infty$  as by our assumptions. Using  $p_{\gamma,c} \rightarrow p$  in  $L^2(\Omega)$ , see theorem 1,  $A_c \subseteq A$  for all  $c > 0$ ,  $p|_{A_c} = 0$  and Hölder's inequality yield

$$\begin{aligned} & \int_{\Omega} |\text{sign}(\bar{\lambda} + c \cdot (y_c - \varphi)) \cdot \nabla \bar{\lambda}^T V \cdot p_c| \, dx \\ & \leq \| \mathbb{1}_{A_c} \cdot p_c \|_{L^2(\Omega)} \cdot \| \nabla \bar{\lambda}^T V \|_{L^2(\Omega)} = \| \mathbb{1}_{A_c} \cdot (p_c - p) \|_{L^2(\Omega)} \cdot \| \nabla \bar{\lambda}^T V \|_{L^2(\Omega)} \\ & \leq \| p_c - p \|_{L^2(\Omega)} \cdot \| \nabla \bar{\lambda}^T V \|_{L^2(\Omega)} \rightarrow 0 \quad \text{for } c \rightarrow \infty, \end{aligned}$$

which is the desired convergence of  $T_0$  to 0.

Next, we proceed in two steps: Firstly, we show convergence for  $T_1$  and  $T_2$  as restricted operators on  $C_0^\infty(\Omega, \mathbb{R}^2)$ . Secondly, we show that the limiting operators can be continuously extended to  $H_0^1(\Omega, \mathbb{R}^2)$ .

Let  $V \in C_0^\infty(\Omega)$ . By this, we have  $\text{div}(V) \cdot p_{\gamma,c}, \nabla \varphi^T V \in H_0^1(\Omega)$  for all  $\gamma, c > 0$ , which enables to use these functions as test functions for the state and adjoint equations. This leads to

$$\begin{aligned} T_1(V) &= -c \cdot \int_{\Omega} \text{sign}_{\gamma}(\bar{\lambda} + c \cdot (y_{\gamma,c} - \varphi)) \cdot \nabla \varphi^T V \cdot p_{\gamma,c} \, dx \\ &= a(p_{\gamma,c}, \nabla \varphi^T V) + (y_{\gamma,c} - \bar{y}, \nabla \varphi^T V)_{L^2(\Omega)} \\ &\rightarrow a(p, \nabla \varphi^T V) + (y - \bar{y}, \nabla \varphi^T V)_{L^2(\Omega)} =: \tilde{T}_1(V) \quad \text{for } \gamma, c \rightarrow \infty \end{aligned}$$

and

$$\begin{aligned} T_2(V) &= \int_{\Omega} \text{div}(V) \cdot \max_{\gamma}(\bar{\lambda} + c \cdot (y_{\gamma,c} - \varphi)) \cdot p_{\gamma,c} \, dx \\ &= -a(y_{\gamma,c}, p_{\gamma,c} \cdot \text{div}(V)) + (f, p_{\gamma,c} \cdot \text{div}(V))_{L^2(\Omega)} \\ &\rightarrow -a(y, p \cdot \text{div}(V)) + (f, p \cdot \text{div}(V))_{L^2(\Omega)} =: \tilde{T}_2(V) \quad \text{for } \gamma, c \rightarrow \infty \end{aligned}$$

due to theorem 1 and proposition 1.

Next, we lift the convergence from  $V \in C_0^\infty(\Omega, \mathbb{R}^2)$  to  $H_0^1(\Omega, \mathbb{R}^2)$  by continuous extension. Since  $C_0^\infty(\Omega, \mathbb{R}^2)$  is a dense subspace of  $H_0^1(\Omega, \mathbb{R}^2)$  and the latter being the completion of the former by the  $\| \cdot \|_{H_0^1(\Omega, \mathbb{R}^2)}$  norm, it is sufficient to show that the limits of  $T_1(V_n)$  and  $T_2(V_n)$  form a Cauchy sequence for a given Cauchy sequence

$(V_n)_{n \in \mathbb{N}} \subset C_0^\infty(\Omega, \mathbb{R}^2)$  under the  $\|\cdot\|_{H_0^1(\Omega, \mathbb{R}^2)}$ -norm. So let  $(V_n)_{n \in \mathbb{N}} \subset C_0^\infty(\Omega, \mathbb{R}^2)$  with  $\|V_n - V_m\|_{H_0^1(\Omega, \mathbb{R}^2)} \rightarrow 0$  for  $m, n \rightarrow \infty$ . For the limit of  $T_1$  we have

$$\begin{aligned}
& |\tilde{T}_1(V_n) - \tilde{T}_1(V_m)| \\
& = |a(p, \nabla \varphi^T(V_n - V_m)) + (y - \bar{y}, \nabla \varphi^T(V_n - V_m))_{L^2(\Omega)}| \\
& \leq \left( \sum_{i,j} \|a_{i,j}\|_{L^\infty(\Omega)} + \sum_j \|d_j\|_{L^\infty(\Omega)} + \|b\|_{L^\infty(\Omega)} \right) \\
& \quad \cdot \int_\Omega \sum_{i,j} \partial_i p \partial_j (\nabla \varphi^T(V_n - V_m)) \\
& \quad + \sum_i (\partial_i p \nabla \varphi^T(V_n - V_m) + p \partial_i \nabla \varphi^T(V_n - V_m)) \\
& \quad + p \nabla \varphi^T(V_n - V_m) dx + \int_\Omega (y - \bar{y}) \nabla \varphi^T(V_n - V_m) dx \\
& = \left( \sum_{i,j} \|a_{i,j}\|_{L^\infty(\Omega)} + \sum_j \|d_j\|_{L^\infty(\Omega)} + \|b\|_{L^\infty(\Omega)} \right) \\
& \quad \cdot \int_\Omega \sum_{i,j} \left( \partial_i p ((\partial_j \nabla \varphi)^T(V_n - V_m) + \nabla \varphi^T \partial_j(V_n - V_m)) \right) \\
& \quad + p \nabla \varphi^T(V_n - V_m) dx + \int_\Omega (y - \bar{y}) \nabla \varphi^T(V_n - V_m) dx \\
& \leq \left( \sum_{i,j} \|a_{i,j}\|_{L^\infty(\Omega)} + \sum_j \|d_j\|_{L^\infty(\Omega)} + \|b\|_{L^\infty(\Omega)} \right) \cdot \|p\|_{H_0^1(\Omega)} \\
& \quad \cdot C \cdot \left( \sum_{i,j} \|(\partial_j \nabla \varphi)^T(V_n - V_m)\|_{L^1(\Omega)} + \|\nabla \varphi^T \partial_j(V_n - V_m)\|_{L^1(\Omega)} \right) \\
& \quad + \|\nabla \varphi^T(V_n - V_m)\|_{L^1(\Omega)} \\
& \quad + C \cdot \|\varphi\|_{H^1(\Omega)} \cdot \|y - \bar{y}\|_{L^2(\Omega)} \cdot \|V_n - V_m\|_{H_0^1(\Omega, \mathbb{R}^2)} \\
& \leq C \cdot \left( \sum_{i,j} \|a_{i,j}\|_{L^\infty(\Omega)} + \sum_j \|d_j\|_{L^\infty(\Omega)} + \|b\|_{L^\infty(\Omega)} \right) \cdot \|p\|_{H_0^1(\Omega)} \\
& \quad \cdot \|\varphi\|_{H^1(\Omega)} \cdot 9 \cdot \|V_n - V_m\|_{H_0^1(\Omega, \mathbb{R}^2)} \\
& \quad + C \cdot \|\varphi\|_{H^1(\Omega)} \cdot \|y - \bar{y}\|_{L^2(\Omega)} \cdot \|V_n - V_m\|_{H_0^1(\Omega, \mathbb{R}^2)} \rightarrow 0 \quad \text{for } m, n \rightarrow \infty.
\end{aligned}$$

Here, we use integration by parts, Gauss' Theorem,  $p|_{\partial\Omega} = 0$ ,  $(V_n - V_m)|_{\partial\Omega} = 0$  the embedding of  $L^2(\Omega)$  into  $L^1(\Omega)$  with constant  $C > 0$ . Thus,  $(\tilde{T}_1(V_n))_{n \in \mathbb{N}}$  forms a Cauchy sequence and, therefore, gives a value for the continuous extension of  $\tilde{T}_1$  for the limit of  $V_n$  in  $H_0^1(\Omega, \mathbb{R}^2)$ . For  $T_2$  we use the same techniques, including the embedding of  $L^2(\Omega)$  into  $L^1(\Omega)$  with constant  $C > 0$ . Then, we achieve

$$\begin{aligned}
& |\tilde{T}_2(V_n) - \tilde{T}_2(V_m)| \\
& = |-a(y, p \cdot \operatorname{div}(V_n - V_m)) + (f, p \cdot \operatorname{div}(V_n - V_m))_{L^2(\Omega)}| \\
& \leq \left( \sum_{i,j} \|a_{i,j}\|_{L^\infty(\Omega)} + \sum_j \|d_j\|_{L^\infty(\Omega)} + \|b\|_{L^\infty(\Omega)} \right) \\
& \quad \cdot 13 \cdot C \cdot \|y\|_{H_0^1(\Omega)} \cdot \|p\|_{H_0^1(\Omega)} \cdot \|V_n - V_m\|_{H_0^1(\Omega, \mathbb{R}^2)} \\
& \quad + C \cdot \|f\|_{L^2(\Omega)} \cdot \|p\|_{H_0^1(\Omega)} \cdot \|V_n - V_m\|_{H_0^1(\Omega, \mathbb{R}^2)} \rightarrow 0 \quad \text{for } m, n \rightarrow \infty.
\end{aligned}$$

With these convergences  $T_1, T_2$  converge to the continuously extended limit objects, which we from now on denote by  $T_1, T_2$ , for all  $V \in H_0^1(\Omega, \mathbb{R}^2)$ . Next, we simplify

the sum of these two limiting objects. Let  $V \in C_0^\infty(\Omega, \mathbb{R}^2)$ . Then

$$\begin{aligned}
& T_1(V) + T_2(V) \\
&= a(p, \nabla\varphi^T V) + (y - \bar{y}, \nabla\varphi^T V)_{L^2(\Omega)} \\
&\quad - a(y, p \cdot \operatorname{div}(V)) + (f, p \cdot \operatorname{div}(V))_{L^2(\Omega)} \\
&= a_{\Omega \setminus A}(p, \nabla\varphi^T V) + (y - \bar{y}, \nabla\varphi^T V)_{L^2(\Omega \setminus A)} \\
&\quad + a_A(p, \nabla\varphi^T V) + (y - \bar{y}, \nabla\varphi^T V)_{L^2(A)} + (\lambda, p \cdot \operatorname{div}(V))_{L^2(\Omega)} \\
&= (\varphi - \bar{y}, \nabla\varphi^T V)_{L^2(A)},
\end{aligned} \tag{35}$$

where we use the definition of  $p$ , complementary slackness of  $\lambda \in L^2(\Omega)$ , test function properties of  $\nabla\varphi^T V$  and  $p \cdot \operatorname{div}(V)$ , the state and adjoint equations. We apply again a continuity argument to gain this identity for all  $V \in H_0^1(\Omega, \mathbb{R}^2)$ . We see that the limit object in (35) is exactly the missing term in the limit of the shape derivatives  $D\mathcal{J}(\Omega)[V]$  (cf. (30)).  $\square$

**Remark 10.** *Theorem 2 and theorem 3 are also valid when  $f \in L^2(\Omega)$  or  $\varphi \in H^2(\Omega)$  depend explicitly on the shape  $\Omega$  with shape derivatives  $f', \varphi' \in H_0^1(\Omega)$ . Then the shape derivatives need to be modified accordingly by replacing terms including  $\nabla f^T V$  and  $\nabla\varphi^T V$  by  $\nabla f^T V + f'$  and  $\nabla\varphi^T V + \varphi'$ . We silently assumed  $f \in L^2(\Omega)$  to be piecewise constant as we do in the numerical section (cf. (40)), without restricting the general proof.*

**Remark 11.** *It is common knowledge that by pushing the obstacle  $\varphi$  to infinity, i.e.,  $\varphi \uparrow \infty$ , the state equation representing the variational inequality (5) becomes a regular elliptic PDE in weak formulation*

$$a(y, v) = (f, v)_{L^2(\Omega)} \quad \forall v \in H_0^1(\Omega)$$

due to (6). This means that we encounter shape optimization problems with elliptic PDE constraints. Formula (30) remains valid by applying  $A = \emptyset$ , giving a shape derivative for a general elliptic problem.

**Remark 12.** *The limiting objects of the convergence results for adjoint variables (cf. theorem 1) and shape derivatives (cf. theorem 2) can be put into relation by conditions resembling  $C$ -stationarity, e.g., as found in [18, Definition 4.1.]. Using our terminology, it is necessary for  $C$ -stationarity conditions to hold that a  $\xi \in H^{-1}(\Omega)$  exists such that the adjoint equation can be formulated in the form*

$$a(p, v) + \langle \xi, v \rangle = -((y - \bar{y}), v)_{L^2(\Omega)}. \tag{36}$$

We can define such a  $\xi \in H^{-1}(\Omega)$  by emulating the definition of  $p$  in (17), including enforcement of the Dirichlet condition  $p = 0$  on  $\partial A$  with Nitsche's method using boundary terms (cf. [23]). The state equation, corresponding complementarity conditions, and the design equation, which in our setting can be viewed as the shape derivative identity (25), hold in analogy to the cited definition of  $C$ -stationarity. The remaining conditions

$$\langle \xi, p \rangle \geq 0 \quad \text{and} \quad p = 0 \quad \text{a.e. in } \{\xi > 0\}, \tag{37}$$

by the definitions of  $\xi$  and  $p$ , are satisfied as well. It is worth mentioning that—no knowledge of the authors—no type of  $C$ -stationarity-like conditions for optimality of VI constrained shape optimization problems have been investigated or defined before. By defining  $C$ -stationarity in this context, as outlined above, we can sum up the theorems by stating that the solutions of the regularized equations converge to a  $C$ -stationary system.

## 4 Algorithmic aspects and numerical investigations

In this section, we put the theoretical treatise highlighted in the previous section into numerical practice. We employ a steepest descent algorithm with backtracking linesearch in order to perform the optimization procedures with various regularized as well as unregularized versions of the specialized variational inequality (see (39)). Also, we propose a way to incorporate the unregularized approach in an algorithm and compare it to the different regularizations.

For convenience, we specialize the more general constraint (5) to a Laplacian version:

$$\min_{\Gamma_{\text{int}}} \frac{1}{2} \int_{\Omega} |y - \bar{y}|^2 dx + \nu \int_{\Gamma_{\text{int}}} 1 ds \quad (38)$$

$$\begin{aligned} \text{s.t.} \quad & \int_{\Omega} \nabla y^T \nabla v dx + \langle \lambda, v \rangle = \int_{\Omega} f v dx \quad \forall v \in H_0^1(\Omega) \\ & \lambda \geq 0 \quad \text{in } \Omega \\ & y \leq \varphi \quad \text{in } \Omega \\ & \lambda(y - \varphi) = 0 \quad \text{in } \Omega \end{aligned} \quad (39)$$

We use  $\nu = 10^{-5}$  for all computations in this section. As the right-hand side of the state equation in eq. (38) we choose the piecewise constant function

$$f(x) = \begin{cases} -10 & \text{for } x \in \Omega_{\text{out}} \\ 100 & \text{for } x \in \Omega_{\text{in}} \end{cases}. \quad (40)$$

For calculations of the smoothed state and adjoint we have to specify  $\max_{\gamma}$  satisfying assumption 1. For demonstrative purpose, we choose a similar smoothing procedure as in [22, Section 2]:

$$\max_{\gamma}(x) = \begin{cases} \max(0, x) & \text{for } x \in \mathbb{R} \setminus [-\frac{1}{\gamma}, \frac{1}{\gamma}] \\ \frac{\gamma}{4}x^2 + \frac{1}{2}x + \frac{1}{4\gamma} & \text{else} \end{cases} \quad (41)$$

A different, more regular smoothing is, e.g., given in [35, (1.10)]. Both smoothing techniques mentioned satisfy assumption 1. For the sake of completeness, we also give the first derivative formula

$$\text{sign}_{\gamma}(x) = \begin{cases} 0 & \text{for } x \in (-\infty, -\frac{1}{\gamma}) \\ \frac{\gamma}{2}x + \frac{1}{2} & \text{for } x \in [-\frac{1}{\gamma}, \frac{1}{\gamma}] \\ 1 & \text{for } x \in (\frac{1}{\gamma}, \infty) \end{cases}. \quad (42)$$

In this setting, the shape derivative (30) simplifies to

$$\begin{aligned} & D\mathcal{J}(\Omega)[V] \\ &= \int_{\Omega} - (y - \bar{y}) \nabla \bar{y}^T V - \nabla y^T (\nabla V^T + \nabla V) \nabla p \\ & \quad + \text{div}(V) \left( \frac{1}{2} (y - \bar{y})^2 + \nabla y^T \nabla p - f p \right) dx + \int_A (\varphi - \bar{y}) \nabla \varphi^T V dx \end{aligned} \quad (43)$$

and analogously the shape derivative for the fully regularized equation in eq. (25). Notice that the shape derivative of the perimeter regularization is also included in our computations (cf. remark 6).

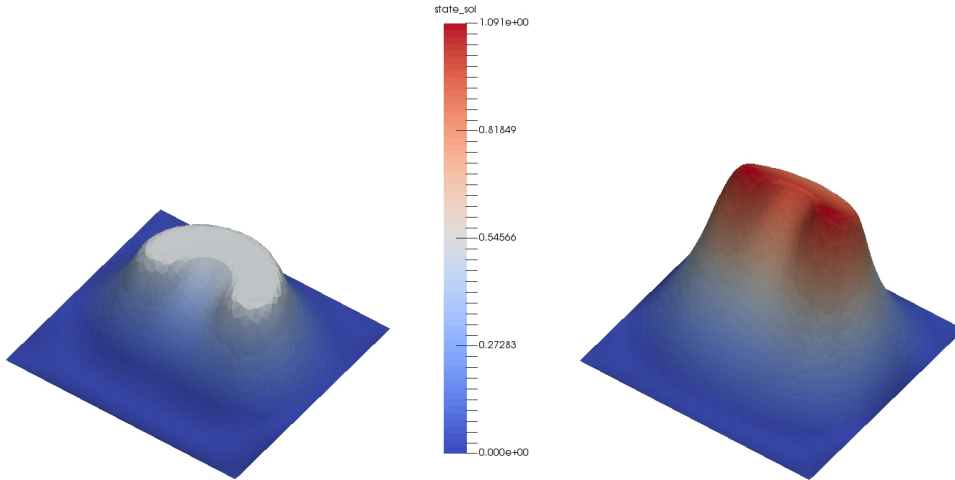


Figure 2: Solutions  $\bar{y}$  to the VI in the target shape. On the left:  $\varphi_1 = 0.5$ . On the right:  $\varphi_2 = 5e^{-x_1-1}$ .

In the following numerical experiments, we consider two different obstacles:

$$\varphi_1(x) = 0.5 \quad \text{and} \quad \varphi_2(x) = 5e^{-x_1-1}. \quad (44)$$

The calculations are performed with Python using the finite element package FEniCS. For detailed informations on FEniCS, we refer to [1] and [29]. As initial shape we choose a centered circle with radius 0.15, illustrated in fig. 6. The computational grid of the initial shape, which is embedded in the hold-all-domain  $(0, 1)^2 \subset \mathbb{R}^2$ , consists of 2 184 vertices with 4 206 cells, having a maximum cell diameter of 0.0359 and a minimum cell diameter of 0.018. The algorithm employed for the shape optimization is summarized in algorithm 2. In the following, we describe the algorithm and the chosen parameters in detail.

The target data  $\bar{y} \in L^2(\Omega)$  is computed by using the mesh of the target interface to calculate a corresponding state solution of eq. (39) by the semi-smooth Newton method proposed in [22]. These are visualized in fig. 2 for both obstacles  $\varphi_1$  and  $\varphi_2$ . We apply the same method for calculating state variables  $y$  in the unregularized optimization approach.

For the regularized and smoothed states  $y_{\gamma,c}$  and  $y_c$  we use a Newton- and semi-smooth Newton method provided by the FEniCS package in order to solve the linear systems assembled by using first order polynomials on the computational grids. All state calculations in our routines are performed with a stopping criterion of  $\varepsilon_{\text{state}} = 3.e - 4$  for the error norms. In light of remark 3 we choose  $\bar{\lambda} = \max\{0, f + \Delta\varphi\}$ , which is possible due to sufficient regularity of  $\varphi_1$  and  $\varphi_2$ .

To ensure assumptions of theorem 1, theorem 2 and theorem 3, it is necessary to fulfill

$$\|\text{sign}_{\gamma}(\bar{\lambda} + c \cdot (y_{\gamma,c} - \varphi)) - \text{sign}(\bar{\lambda} + c \cdot (y_c - \varphi))\|_{L^1(\Omega)} \rightarrow 0 \quad \text{for } \gamma \rightarrow \infty. \quad (45)$$

We calculate the corresponding norm using various  $c > 0$  and both,  $\varphi_1$  and  $\varphi_2$ , on refined meshes having 212 642 vertices, 423 682 cells and maximum and minimum cell diameter of 0.0038 and 0.0015, respectively. An example convergence plot can be found in fig. 3. We want to point out that as  $\gamma \rightarrow \infty$ , the norm in (45) converges to an  $\varepsilon > 0$  which is close to 0. This is due to numerical errors resulting from if-else

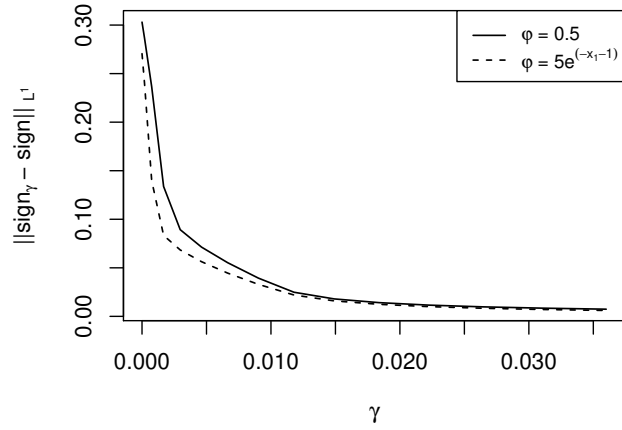


Figure 3: Convergence plots for  $\|\text{sign}_\gamma(\bar{\lambda} + c \cdot (y_{\gamma,c} - \varphi)) - \text{sign}(\bar{\lambda} + c \cdot (y_c - \varphi))\|_{L^1(\Omega)}$ .

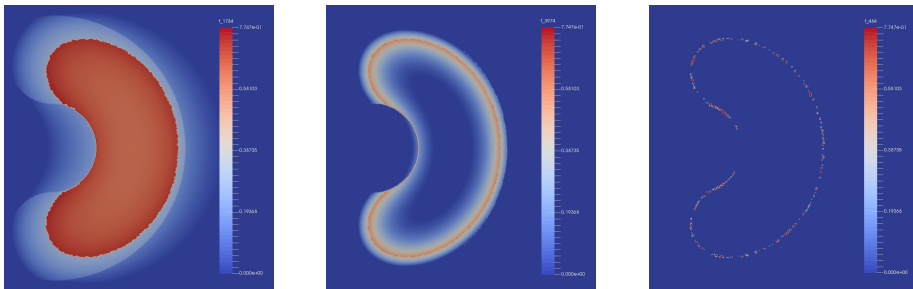


Figure 4: Graphs of  $\text{sign}_\gamma(\bar{\lambda} + c \cdot (y_{\gamma,c} - \varphi)) - \text{sign}(\bar{\lambda} + c \cdot (y_c - \varphi))$  as functions of  $x \in \Omega$  calculated on the refined target mesh with  $c = 1000$ . From left to right:  $\gamma = 0.00075$ ,  $\gamma = 0.009$  and  $\gamma = 10$ .

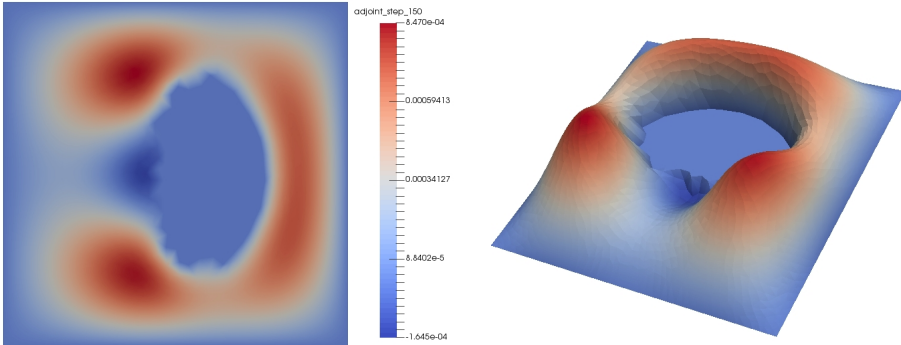


Figure 5: Solution of the adjoint  $p$  in step 150 for the unregularized equation (17) and  $\varepsilon_{\text{adj}} = 10^{-9}$ .

operations to calculate the values of  $\text{sign}$  and  $\text{sign}_\gamma$ , which are illustrated in fig. 4 on the refined mesh. Furthermore, we observe that the errors go to 0 for ever finer grid widths.

The adjoints  $p_{\gamma,c}$  and  $p_c$  are calculated by solving eq. (10) and eq. (16) with first order elements by using the FEniCS standard linear algebra back end solver PETSc.

Calculating the limit  $p$  of the adjoints  $p_{\gamma,c}$  as in eq. (17) and eq. (18) are performed in several steps. First, a linear system corresponding to

$$\begin{aligned} -\Delta p &= -(y - \bar{y}) & \text{in } \Omega \\ p &= 0 & \text{on } \partial\Omega \end{aligned} \quad (46)$$

is assembled without incorporation of information from the active set  $A$ . Afterwards, the vertex indices corresponding to the points in the active set  $A = \{x \in \Omega \mid y - \varphi \geq 0\}$  are collected by checking the condition

$$y(x) - \varphi(x) \geq -\varepsilon_{\text{adj}} \quad (47)$$

for some error bound  $\varepsilon_{\text{adj}} > 0$ . The error bound  $\varepsilon_{\text{adj}}$  is incorporated since  $y$  is feasibly approximated by  $y_i$  with the semi-smooth Newton method from [22], i.e.,  $y_i \leq \varphi$  for all  $i \in \mathbb{N}$ . After this, the collected vertex indices are used to incorporate the Dirichlet boundary conditions  $p = 0$  in  $A$  into the linear system corresponding to (46). To solve the resulting system, we use the same procedures as to solve for  $p_{\gamma,c}, p_c$ , i.e. the standard PETSc back end conjugate gradient solver. An exemplary solution  $p$  of the unregularized adjoint equation is illustrated in fig. 5. We want to point out that the active set and consequently the zero level set resulting from the Dirichlet conditions can be observed in fig. 5.

To calculate gradients  $U \in H_0^1(\Omega, \mathbb{R}^2)$  used in the steepest descent method for solving eq. (38), we use a Steklov-Poincaré metric induced by the linear elasticity equation, as proposed in [36]. In particular, we assemble the shape derivatives given

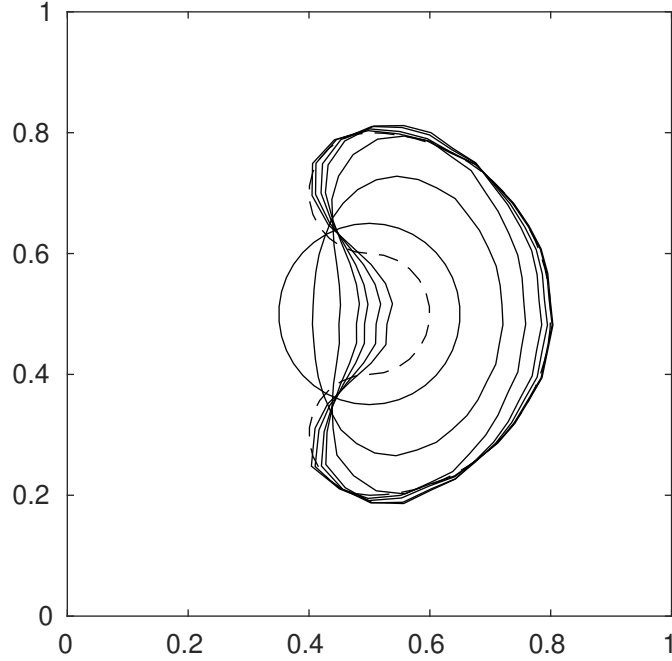


Figure 6: Interfaces of steps 0, 50, 150, 320, 450, 750, 1200 of the unregularized optimization procedure using  $\varepsilon_{\text{adj}} = 10^{-9}$  and  $\varphi_2 = 5e^{-x_1-1}$ . The target interface is represented with dotted lines, the start interface is the centered circle.

in theorem 2 and theorem 3 as the right-hand side of the linear elasticity equation

$$\begin{aligned}
 \int_{\Omega} \sigma(U) : \epsilon(V) \, dx &= DJ(\Omega)[V] \quad \forall V \in H_0^1(\Omega, \mathbb{R}^2) \\
 \sigma(U) &:= \lambda_{\text{elas}} \text{Tr}(U)I + 2\mu_{\text{elas}}\epsilon(U) \\
 \epsilon(U) &:= \frac{1}{2}(\nabla U^T + \nabla U) \\
 \epsilon(V) &:= \frac{1}{2}(\nabla V^T + \nabla V)
 \end{aligned} \tag{48}$$

with the so called Lamé-parameters  $\lambda_{\text{elas}}$  and  $\mu_{\text{elas}}$ . Here, we choose  $\lambda_{\text{elas}} = 0$  and  $\mu_{\text{elas}}$  as the solution of the Poisson problem

$$\begin{aligned}
 -\Delta \mu_{\text{elas}} &= 0 && \text{in } \Omega \\
 \mu_{\text{elas}} &= \mu_{\text{max}} && \text{on } \Gamma \\
 \mu_{\text{elas}} &= \mu_{\text{min}} && \text{on } \partial\Omega
 \end{aligned} \tag{49}$$

for  $\mu_{\text{max}}, \mu_{\text{min}} > 0$ . As a physical interpretation, this enables to control stiffness of the grid by choosing  $\mu_{\text{max}}$  and  $\mu_{\text{min}}$  in order to influence  $\mu_{\text{elas}}$  acting as a coefficient function in the linear elasticity equation (48). Thus, larger values of  $\mu_{\text{max}}$  lead to more stiffness at the interface  $\Gamma$  and larger values of  $\mu_{\text{min}}$  to more stiffness at the boundary  $\partial\Omega$  of the hold-all domain  $\Omega$ . For our calculations, we choose  $\mu_{\text{min}} = 0$  and  $\mu_{\text{max}} = 25$  for  $\varphi_1$  and  $\mu_{\text{max}} = 55$  for  $\varphi_2$ . It is important to notice that we set all right-hand side values of (48) which do not have a neighboring vertex on the interface to 0. For a more detailed discussion of this we refer to [36].

To complete the description of our optimization we shortly explain the line-search we will employ in our numerical calculations. We use a simple backtracking

linesearch with sufficient descent criterion, where  $U_k$  denotes the shape derivative calculated at the corresponding interface in  $\Omega_k$  in step number  $k$ ,  $\mathcal{T}_{\tilde{U}}(\Omega_k) := \{y \in \mathbb{R}^2 : y = x + \tilde{U}(x) \text{ for some } x \in \Omega_k\}$  the linearized vector transport by  $\tilde{U}$  and  $y_{\tilde{U}}$  the state solution in  $\mathcal{T}_{\tilde{U}}(\Omega_k)$ .

```

1  $\tilde{U} \leftarrow U_k$ 
2 while  $\mathcal{J}(y_{\tilde{U}}, \mathcal{T}_{\tilde{U}}(\Omega_k)) > 0.995 \cdot \mathcal{J}(y_k, \Omega_k)$  do
3   |  $\tilde{U} \leftarrow 0.5 \cdot \tilde{U}$ 
4 end
5  $\Omega_{k+1} \leftarrow \mathcal{T}_{\tilde{U}}(\Omega_k)$ 

```

**Algorithm 1:** Backtracking linesearch.

We summarize our approach in algorithm 2 for the unregularized procedures. The regularized and smoothed procedures work analogously by modifying the state, adjoint and shape derivative equations. The calculations of  $p_{\gamma,c}, p_c$  are straightforward and need not the additional steps outlined in before and in algorithm 2 for the unregularized  $p$ .

```

1 Set  $\Omega_0, \varphi, f, \bar{\lambda}, \bar{y}$ 
2 while  $\|D\mathcal{J}(\Omega_k)\| > \varepsilon_{\text{shape}}$  do
3   Calculate state  $y_k$  with tolerance  $\varepsilon_{\text{state}}$ 
4   Calculate adjoint  $p_k$ 
5     Assemble adjoint system (46) neglecting active set
6     Collect vertex indices of active set by (47)
7     Implement Dirichlet conditions of active set
8     Solve modified adjoint linear system
9   Calculate shape gradient  $\tilde{U}_k$ 
10    Assemble gradient system (48)
11    Set  $D\mathcal{J}(\Omega_k)[V] = 0$  on all vertices without support at interface  $\Gamma_{\text{int}}$ 
12    Solve for gradient  $U_k$ 
13    Perform backtracking linesearch (algorithm 1) to get  $\tilde{U}_k$ 
14     $\Omega_{k+1} \leftarrow \mathcal{T}_{\tilde{U}_k}(\Omega_k)$ 
15 end

```

**Algorithm 2:** Shape optimization for unregularized VI constraints.

Our findings concerning convergence of the various shape optimization approaches, using the unregularized approach for various  $\varphi_{\text{adj}}$ , as well as regularized approaches with different parameters  $\gamma, c > 0$ , are displayed in fig. 7 for  $\varphi_1 = 0.5$  and in fig. 8 for  $\varphi_2 = 5e^{-x_1-1}$ . Morphed shapes arising during the optimization procedure are plotted in fig. 6 for the unregularized approach using  $\varepsilon_{\text{adj}} = 10^{-9}$ . It can be seen in the plots that there are vanishing difference between approaches using fully regularized calculation with sufficiently high  $\gamma$  and  $c$ , regularized ones with high  $c$  and the unregularized one. For smaller regularization parameters  $\gamma$  and  $c$ , the solved state and adjoint equations begin to differ from the original problem and, thus, slowing down convergence, and for very low  $\gamma$  and  $c$  no convergence at all.

The convergence behavior of the unregularized method strongly depends on the selection of the active set. When the state solution  $y$  is not calculated with sufficient precision the numerical errors lead to misclassification of vertex indices. Hence wrong Dirichlet conditions are incorporated in the adjoint system, creating errors in the adjoint. This makes the gradient sensitive to error for smaller  $\varepsilon_{\text{adj}}$ , as can be seen by the slight roughness of the target graphs in fig. 7 and fig. 8 for  $\varepsilon_{\text{adj}} = 10^{-9}$  and  $\varepsilon_{\text{adj}} = 0.01$ . In order to compensate this, the condition for checking active set indices (47) can be relaxed by increasing  $\varepsilon_{\text{adj}}$ . This increases likelihood

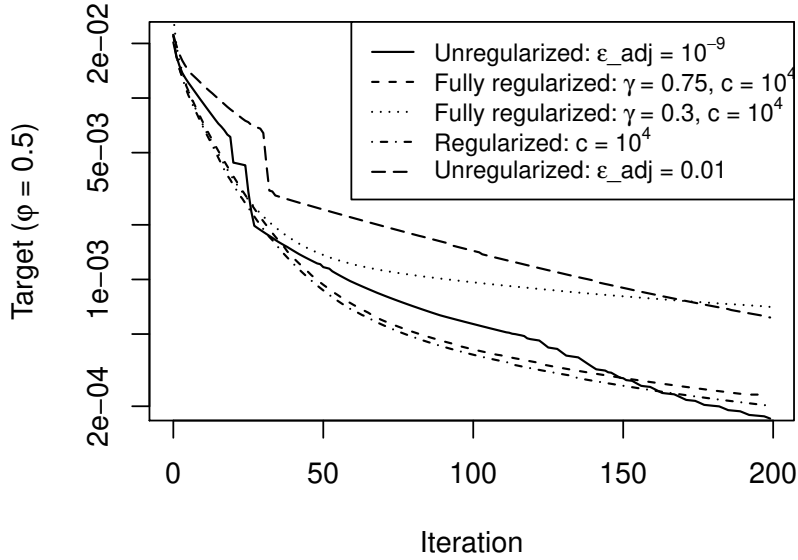


Figure 7: Convergence plot for the different regularization and unregularized approaches for obstacle  $\varphi_1 = 0.5$

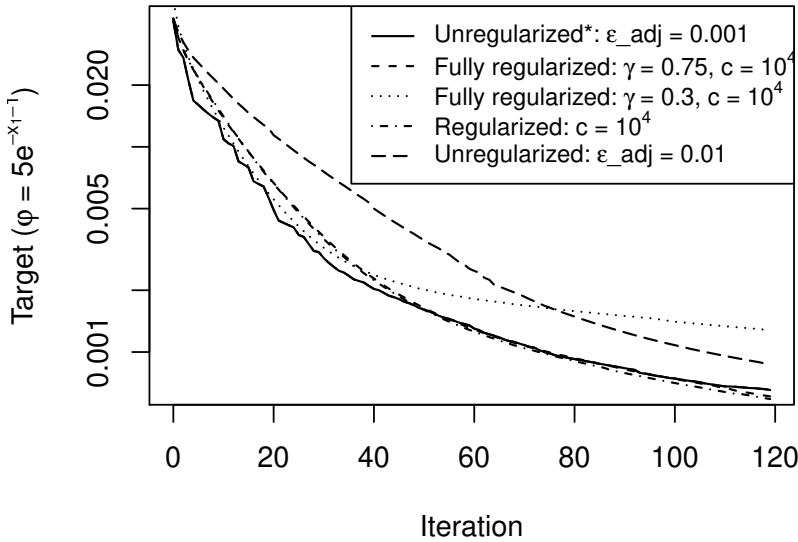


Figure 8: Convergence plot for the different regularization and unregularized approaches for obstacle  $\varphi_2 = 5e^{-x_1-1}$ . Unregularized\* uses a lower tolerance  $\epsilon_{\text{state}} = 0.00001$  for the state calculation. Notice that regularized and fully regularized approaches for  $\gamma = 0.75, c = 10^4$  are almost indistinguishable.

of correctly classifying the true active indices, while also increasing likelihood of misclassification of inactive indices. Such a relaxation can lead to errors in the adjoint increasing with  $\varepsilon_{\text{adj}}$  and, thus, trading convergence speed for robustness, also visible in fig. 7 and fig. 8. Of course, this gets less feasible for highly oscillatory obstacle  $\varphi$  and state  $y$ , as well as state solves with high tolerance  $\varepsilon_{\text{state}}$ .

In order to circumvent this, it is obviously sufficient to decrease error tolerance  $\varepsilon_{\text{state}}$  of the state calculation. An exemplary result of this can be seen in fig. 8 under unregularized\*, where we decreased the error tolerance to  $\varepsilon_{\text{state}} = 4.e - 5$ . Nevertheless, additional decrease of  $\varepsilon_{\text{state}}$  comes with more computational cost, whereas with increase of  $\varepsilon_{\text{adj}}$  the robustness is paid by loss of convergence speed.

It is worth to mention that implementing the unregularized state and adjoint becomes especially numerically exploitable with higher resolution meshes and more strongly binding obstacles  $\varphi$ , i.e., larger active sets  $A$ . This is possible by sparse solvers due to the incorporation of Dirichlet conditions on the active set, as we have proposed, or by a fat boundary method as in [30].

So in contrast to the method proposed in [14], where performance slows down for more active obstacle  $\varphi$ , we do not notice unusual slowdown in performance with the methods proposed in this article, and even offer possibility to actually benefit numerically from more binding obstacle  $\varphi$ .

## 5 Conclusion

Shape optimization for variational inequalities is more challenging than both, elliptic shape optimization and optimal control for variational inequalities. In this paper, we derive optimality conditions for shape optimization in the context of variational inequalities in the flavor of optimal control problems. Regularized variants are studied and limiting conditions derived. This gives rise to highly efficient optimization algorithms. In the future general investigations of necessary optimality criteria for VI constrained shape optimization like C-stationarity are conceivable. Also large-scale multidimensional computational comparisons of the presented method in comparison to other state-of-the-art methods is of particular interest.

## Acknowledgement

The authors are indebted to Leonhard Frerick (Trier University) for many helpful comments and discussions about functional analytical aspects of convergence. Furthermore, the paper profited from remarks of Gerd Wachsmuth on an earlier version. This work has been partly supported by the German Research Foundation (DFG) within the priority program SPP 1962 “Non-smooth and Complementarity-based Distributed Parameter Systems: Simulation and Hierarchical Optimization” under contract number Schu804/15-1, by the DFG research training group 2126 Algorithmic Optimization, and by the BMBF (Bundesministerium für Bildung und Forschung) within the collaborative project GIVEN (FKZ: 05M18UTA).

## References

- [1] M. S. Alnæs, J. Blechta, J. Hake, A. Johansson, B. Kehlet, A. Logg, C. Richardson, J. Ring, M. E. Rognes, and G. N. Wells. The FEniCS project version 1.5. *Archive of Numerical Software*, 3(100), 2015.
- [2] H. B. Amour, M. Burger, and B. Hackl. Level Set Methods for Geometric Inverse Problems in Linear Elasticity. *Inverse Problems*, 20(3):673–696, 2004.

- [3] M. Berggren. A Unified Discrete–Continuous Sensitivity Analysis Method for Shape Optimization. In *Applied and Numerical Partial Differential Equations*, volume 15 of *Computational Methods in Applied Sciences*, pages 25–39. Springer, 2010.
- [4] J.F. Bonnans and D. Tiba. Pontryagin’s Principle in the Control of Semilinear Elliptic Variational Inequalities. *Applied Mathematics and Optimization*, 23(1):299–312, 1991.
- [5] H. Brézis. Monotonicity Methods in Hilbert Spaces and Some Applications to Nonlinear Partial Differential Equations. *Contributions to Nonlinear Functional Analysis*, pages 101–156, 1971.
- [6] H. Brézis and G. Stampacchia. Sur la régularité de la solution d’inéquations elliptiques. *Bulletin de la Société Mathématique de France*, 96:153–180, 1968.
- [7] C. Christof, C. Clason, C. Meyer, and S. Walther. Optimal Control of a Non-Smooth Semilinear Elliptic Equation. *Mathematical Control & Related Fields*, 8(1):247–276, 2018.
- [8] R. Correa and A. Seeger. Directional derivative of a minmax function. *Nonlinear Analysis: Theory, Methods & Applications*, 9(1):13–22, 1985.
- [9] G. Stampacchia D. Kinderlehrer. *An Introduction to Variational Inequalities and Their Applications*, volume 31. SIAM, 1980.
- [10] M.C. Delfour and J.-P. Zolésio. Shape Sensitivity Analysis via Min Max Differentiability. *SIAM Journal on Control and Optimization*, 26(4):834–862, 1988.
- [11] M.C. Delfour and J.-P. Zolésio. *Shapes and Geometries: Metrics, Analysis, Differential Calculus, and Optimization*, volume 22 of *Advances in Design and Control*. SIAM, 2nd edition, 2001.
- [12] Z. Denkowski and S. Migorski. Optimal Shape Design for Hemivariational Inequalities. *Universitatis Iagellonicae Acta Mathematica*, 36:81–88, 1998.
- [13] L.C. Evans. *Partial Differential Equations*. American Mathematical Society, 1993.
- [14] B. Führ, V.H. Schulz, and K. Welker. Shape Optimization for Interface Identification with Obstacle Problems. *Vietnam Journal of Mathematics*, 2018. DOI: 10.1007/s10013-018-0312-0.
- [15] L. Gasiński. Mapping Method in Optimal Shape Design Problems Governed by Hemivariational Inequalities. In J. Cagnol, M. Polis, and J.-P. Zolésio, editors, *Shape Optimization And Optimal Design*, number 216, pages 277–288. New York; Marcel Dekker, 2001.
- [16] C. Heinemann and K. Sturm. Shape Optimization for a Class of Semilinear Variational Inequalities with Applications to Damage Models. *SIAM Journal on Mathematical Analysis*, 48(5):3579–3617, 2016.
- [17] M. Hintermüller. An Active-Set Equality Constrained Newton Solver with Feasibility Restoration for Inverse Coefficient Problems in Elliptic Variational Inequalities. *Inverse Problems*, 24(3):034017, 2008.
- [18] M. Hintermüller and I. Kopacka. Mathematical Programs with Complementarity Constraints in Function Space: C- and Strong Stationarity and a Path-Following Algorithm. *SIAM Journal on Optimization*, 20(2):868–902, 2009.

- [19] M. Hintermüller and L. Laurain. Optimal Shape Design Subject to Elliptic Variational Inequalities. *SIAM Journal on Control and Optimization*, 49(3):1015–1047, 2011.
- [20] M. Hintermüller and T. Surowiec. First-Order Optimality Conditions for Elliptic Mathematical Programs with Equilibrium Constraints via Variational Analysis. *SIAM Journal on Optimization*, 21(4):1561–1593, 2011.
- [21] K. Ito and K. Kunisch. Optimal Control of Elliptic Variational Inequalities. *Applied Mathematics and Optimization*, 41(3):343–364, 2000.
- [22] K. Ito and K. Kunisch. Semi-Smooth Newton Methods for Variational Inequalities of the First Kind. *ESIAM: Mathematical Modelling and Numerical Analysis*, 37:41–62, 2003.
- [23] M. Juntunen and R. Stenberg. Nitsches Method for General Boundary Conditions. *Mathematics of Computation*, 78(267):1353–1374, 2009.
- [24] K. Sturm. On shape optimization with non-linear partial differential equations. 2015.
- [25] M. Kocvara and J. Outrata. Shape Optimization of Elasto-Plastic Bodies Governed by Variational Inequalities. In J.-P. Zolésio, editor, *Boundary Control and Variation*, number 163 in Lecture Notes in Pure and Applied Mathematics, pages 261–271. Marcel Dekker, 1994.
- [26] J. L. Lions and G. Stampacchia. Variational Inequalities. *Communications on Pure and Applied Mathematics*, 20:493–519, 1967.
- [27] W.B. Liu and J.E. Rubio. Optimal shape design for systems governed by variational inequalities, part 1: Existence theory for the elliptic case. *Journal of Optimization Theory and Applications*, 69(2):351–371, 1991.
- [28] W.B. Liu and J.E. Rubio. Optimal shape design for systems governed by variational inequalities, part 2: Existence theory for the evolution case. *Journal of Optimization Theory and Applications*, 69(2):373–396, 1991.
- [29] A. Logg, K.-A. Mardal, G. N. Wells, et al. *Automated Solution of Differential Equations by the Finite Element Method*. Springer, 2012.
- [30] B. Maury. A Fat Boundary Method for the Poisson Problem in a Domain with Holes. *Journal of Scientific Computing*, 16(3):319–339, 2001.
- [31] A. Myśliński. Domain Optimization for Unilateral Problems by an Embedding Domain Method. In J. Cagnol, M. Polis, and J.-P. Zolésio, editors, *Shape Optimization And Optimal Design*, number 216 in Lecture Notes in Pure and Applied Mathematics, pages 355–370. Marcel Dekker, 2001.
- [32] A. Myśliński. Level Set Approach for Shape Optimization of Contact Problems. In P. Neittaanmäki, T. Rossi, K. Majava, O. Pironneau, and I. Lasiecka, editors, *European Congress on Computational Methods in Applied Sciences and Engineering ECCOMAS*, 2004.
- [33] A. Myśliński. Level Set Method for Shape and Topology Optimization of Contact Problems. In *IFIP Conference on System Modeling and Optimization*, pages 397–410. Springer, 2007.
- [34] A. Novotny and J. Sokolowski. *Topological Derivatives in Shape Optimization*. Springer, 2013.

- [35] A. Schiela and D. Wachsmuth. Convergence Analysis of Smoothing Methods for Optimal Control of Stationary Variational Inequalities. *ESAIM: Mathematical Modelling and Numerical Analysis*, 47(3):771–787, 2013.
- [36] V.H. Schulz, M. Siebenborn, and K. Welker. Efficient PDE Constrained Shape Optimization based on Steklov-Poincaré Type Metrics. *SIAM Journal on Optimization*, 26(4):2800–2819, 2016.
- [37] M. Siebenborn and K. Welker. Algorithmic Aspects of Multigrid Methods for Optimization in Shape Spaces. *SIAM Journal on Scientific Computing*, 39(6):B1156–B1177, 2017.
- [38] J. Sokolowski and J.-P. Zolésio. *Introduction to Shape Optimization*, volume 16 of *Computational Mathematics*. Springer, 1992.
- [39] K. Sturm. Shape differentiability under non-linear PDE constraints. In A. Pratelli and G. Leugering, editors, *New Trends in Shape Optimization*, volume 166 of *International Series of Numerical Mathematics*, pages 271–300. Springer, 2015.
- [40] R. Temam and I. Ekeland. *Analyse convexe et problemes variationnels*. Springer, 1974.
- [41] G.M. Troianiello. *Elliptic Differential Equations and Obstacle Problems*. Springer Science & Business Media, 2013.
- [42] K. Welker. *Efficient PDE Constrained Shape Optimization in Shape Spaces*. PhD thesis, Universität Trier, 2016.
- [43] K. Welker. Suitable Spaces for Shape Optimization. *arXiv:1702.07579*, 2017. <https://arxiv.org/abs/1702.07579>.
- [44] E. Zeidler. *Applied Functional Analysis: Main Principles and Their Applications*, volume 109. Springer Science & Business Media, 2012.